1249986
[0064843H]

RPP-RPT-47486, Rev. 0

Surface Geophysical Exploration of UPR-200-E-86 Near the C Tank Farm

Prepared by **Dale Rucker, Columbia Energy and Environmental Services, Inc.** for
Washington River Protection Solutions
Richland, WA 99352
U.S. Department of Energy Contract DE-AC27-08RV14800

EDT/ECN: DRF UC:
Cost Center: Charge Code:
B&R Code: Total Pages: 54

Key Words: Surface geophysical exploration, C Farm, Resistivity

RECEIVED
AUG 22 2018
EDMC

Abstract: The report documents the results of a resistivity survey conducted around UPR-200-E-86 in the C tank farm.

TRADEMARK DISCLAIMER. Reference herein to any specific commercial product, process, or service by trade name, trademark, manufacturer, or otherwise, does not necessarily constitute or imply its endorsement, recommendation, or favoring by the United States Government or any agency thereof or its contractors or subcontractors.

SEP 10 2010
DATE:
STA: 15
HANFORD RELEASE
ID: 3

Nancy A Fouad 9-10-10
Release Approval Date

Release Stamp

Approved For Public Release

EXECUTIVE SUMMARY

This report documents electrical geophysics exploration activities completed within a 78-meter by 66-meter area surrounding the UPR-200-E-86 unplanned release (UPR-86) site in the vicinity of the C tank farm. hydroGEOPHYSICS, Inc. and Columbia Energy and Environmental Services, Inc., with support from technical staff of Washington River Protection Solutions, LLC, conducted a geophysical survey of the UPR-86 with the objective of analyzing electrical resistivity data to locate low resistivity targets that may be indicative of increased soil moisture or salts from the unplanned release.

Three-dimensional data acquisition of high-resolution electrical resistivity data were acquired at 301 surface electrodes (located at the ground surface) and five depth electrodes. The depth electrodes were used to improve the target resolution in the area below the localized surface infrastructure. The data were inverse modeled with a multi-threaded algorithm capable of handling large domains, called RES3DINVx64. The use of a multi-threaded code allows faster modeling times over single threaded codes.

Results from the analyses of more than thirty separate inverse models showed that the area beneath UPR-86 was relatively resistive despite the 17,000-gallon projected release. Small isolated conductive targets are seen in the area, which may be more reminiscent of noise than actual subsurface features. When the data from the adjacent UPR-81 site was combined with the UPR-86 data and both areas inverse modeled together, stark differences in the distribution of electrical resistivity were observed. Figure ES-1 shows the results of the combined sites, and the UPR-81 site is much more electrically conductive, despite having released only about twice as much (36,000 gallons) to the subsurface.

The findings of the resistivity survey combined with the soil sampling analyses from probeholes surrounding the release site suggest that the 17,000-gallon release may have been an over estimate. The 17,000 value could have been estimated by a 20-foot by 20-foot by 20-foot block of soil with 30 percent of the space filled by the release, i.e., all of the pore space was filled by the release. This, also, is unlikely given that some layers within the soil are already at 20 to 25 percent moisture. Other, less likely explanations for the resistivity and soil sampling results include a release that has been sufficiently diluted over time or a release of low ionic strength.

Figure ES-1. Distribution of Calculated Resistivity for the UPR-81 and UPR-86 Sites.

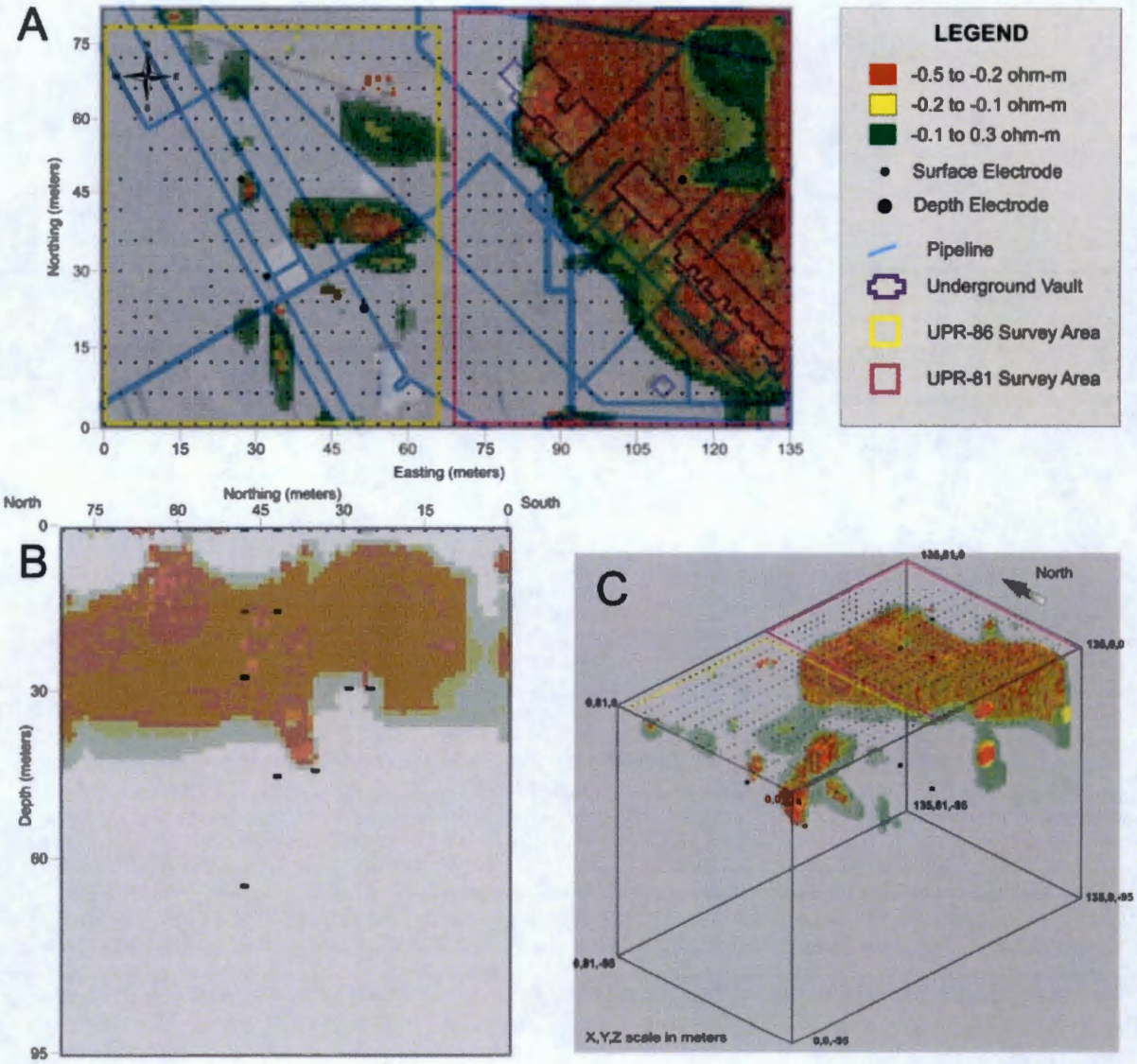

(A) Plan view.
(B) Side view, looking east.
(C) Oblique view, looking northeast.

TABLE OF CONTENTS

1.0 INTRODUCTION 1-1
- 1.1 SCOPE 1-1
- 1.2 OBJECTIVES 1-1
- 1.3 REPORT LAYOUT 1-1

2.0 BACKGROUND 2-2
- 2.1 TANK FARM FACILITIES AND INFRASTRUCTURE 2-5
- 2.2 UNPLANNED RELEASES 2-6
- 2.3 SOIL SAMPLING AT UPR-86 2-6

3.0 QUALITY ASSURANCE 3-1
- 3.1 CALIBRATION AND MAINTENANCE OF EQUIPMENT AND INSTRUMENTS 3-1
- 3.2 DATA COLLECTION 3-2
- 3.3 ELECTRICAL INTERFERENCE MONITORING 3-2
- 3.4 EQUIPMENT TESTING 3-4
  - 3.4.1 SuperSting 3-4
  - 3.4.2 Switchboxes 3-4
- 3.5 DATA PROCESSING 3-5

4.0 DATA ACQUISITION AND PROCESSING METHODOLOGY 4-1
- 4.1 SURVEY DESIGN 4-1
- 4.2 EQUIPMENT 4-3
  - 4.2.1 ELECTRODE AND CABLE LAYOUT 4-3
  - 4.2.2 RESISTIVITY METER 4-4
- 4.3 ACQUISITION METHODOLOGY 4-5
- 4.4 DATA PROCESSING 4-5
  - 4.4.1 Data Reduction 4-5
  - 4.4.2 Depth Electrode Data Analysis 4-7
  - 4.4.3 3D Inverse Modeling 4-9
  - 4.4.4 Inversion Model Parameters 4-10

5.0 RESULTS 5-1
- 5.1 INVERSE MODELING RESULTS 5-1
  - 5.1.1 UPR-86 Results 5-1
  - 5.1.2 Combined UPR-86 and UPR-81 Data 5-7
- 5.2 MODELING PERFORMANCE 5-14

6.0 CONCLUSIONS 6-1

7.0 REFERENCES 7-1

LIST OF FIGURES

2-1. Location Map of Waste Management Area C in the 200 East Area of the Hanford Site. 2-3
2-2. Map of the C Tank Farm and Surrounding Facilities 2-4
2-3. Map of the C Tank Farm and Surrounding Facilities 2-5
2-4. Probehole sampling at UPR-81 and UPR-86 2-8
2-5. Sulfate and Nitrate Mass Concentrations for UPR-81 and UPR-86 2-9
3-1. Example of Electrical Interference Monitoring 3-3
4-1. Electrode Layout and the Local Distribution of Infrastructure for the UPR-200-E-86 Survey Area 4-2
4-2. Resistivity Data Acquisition System 4-4
4-3. Forward and Reverse Data Sets (Raw Data) 4-6
4-4. Forward and Reverse Data Sets after Data Editing 4-7
4-5. Depth Electrode Histogram Analysis for UPR-E-86 Showing Analysis of (A) V/I Data, (B) Current Values, and (C) Error Values 4-8
4-6. Flowchart of the Resistivity Inversion Process 4-10
5-1. Distribution of Calculated Resistivity for Inverse Model 001 5-2
5-2. Plan View Depth Slices of Distribution of Calculated Resistivity for Inverse Model 001 5-3
5-3. Distribution of Calculated Resistivity for Inverse Model 019 5-5
5-4. Plan View Depth Slices of Distribution of Calculated Resistivity for Inverse Model 019 5-6
5-5. Electrode Distribution for the UPR-81 and UPR-86 Resistivity Projects 5-7
5-6. Histogram Comparison of the Raw Data for UPR-86 and UPR-81 5-8
5-7. Distribution of Calculated Resistivity for Inverse Model 024 5-10
5-8. Plan View Depth Slices of Distribution of Calculated Resistivity for Inverse Model 024 5-11
5-9. Distribution of Calculated Resistivity for Inverse Model 025 5-12
5-10. Plan View Depth Slices of Distribution of Calculated Resistivity for Inverse Model 025 5-13
5-11. Model 001 Convergence Curve 5-14
5-12. Model 019 Convergence Curve 5-15
5-13. Model 024 Convergence Curve 5-15
5-14. Model 025 Convergence Curve 5-16

LIST OF TABLES

4-1. Subsurface (Depth) Electrodes Placed around UPR-200-E-86 4-3
4-2. Number of Data Points Retained During Data Editing Steps 4-7
5-1. Inverse Modeling Convergence and Error Statistics Table 5-16

LIST OF TERMS

Δm	modeled resistivity
2D	two-dimensional
3D	three-dimensional
AGI	Advanced Geosciences, Inc.
bgs	below ground surface
EarthImager3DCL®	EI3DCL
RMS	root-mean-square
SBDT	switchbox diagnostic tester
SGE	surface geophysical exploration
STS	surface-to-surface
UPR	unplanned release
V/I	resistance

Units

g/L	gram per liter
mA	milliamp
ug/g	microgram/gram

® EarthImager3DCL is a registered trademark of Advanced Geosciences, Inc.

1.0 INTRODUCTION

This report documents surface geophysical exploration (SGE) activities completed within a 78-meter by 66-meter area surrounding the UPR-86 site in the vicinity of the C tank farm at the U.S. Department of Energy Hanford Site in Washington State in fiscal year 2010. hydroGEOPHYSICS, Inc. and Columbia Energy and Environmental Services, Inc., with support from technical staff of Washington River Protection Solutions, LLC, conducted a three-dimensional (3D) survey of the subsurface using electrical resistivity. Data acquisition and analysis were performed in accordance with RPP-PLAN-39364, *Work Plan for Surface Geophysical Exploration of UPRs near the C Tank Farm.* High-resolution electrical resistivity data were acquired using both surface electrodes (located at the ground surface) and five depth electrodes completed within the UPR-86 footprint.

1.1 SCOPE

The scope of this electrical resistivity characterization survey included:

- Data acquisition on both surface electrodes and depth electrodes
- Data processing that included the use of methods and controls to ensure quality in the processing and reduction of data collected
- Data visualization that included contouring of resistivity data from the 3D acquired data set
- Compilations of 3D resistivity cross sections.

The UPR-86 is immediately west and adjacent to UPR-81, which was investigated in 2009 using electrical resistivity (RPP-RPT-41236, *Surface Geophysical Exploration of UPR 200-E-81 Near the C Tank Farm*). Given the proximity of the two sites, resistivity data from both were combined and modeled to develop a more complete understanding of the two sites.

1.2 OBJECTIVES

The main objective for this geophysical investigation was to collect and analyze electrical resistivity data to identify low resistivity regions in and around the UPR-86 site in the vicinity of the C tank farm area. Low resistivity measurements are indicative of increased moisture content, changes in geologic composition or formations, or increased concentration of electrolytes compared to background conditions.

1.3 REPORT LAYOUT

The overall scope and content of this report is divided into several main sections as follows:

- **Section 1.0, Introduction** – Describes the scope and objectives of the investigation.

- **Section 2.0, Background** – Describes the setting and information regarding the C tank farm and the UPR-200-E-86 UPR site.
- **Section 3.0, Quality Assurance and Control**
- **Section 4.0, Data Acquisition and Processing** – Presents general layout of the data acquisition and processing with methods and controls used to ensure the quality and control of data collection, reduction, and processing used in this study.
- **Section 5.0, Results and Interpretations** – Presents the results from the electrical resistivity surveying effort and an interpretation of the resistivity measurements including the results of the inversion analysis.
- **Section 6.0, Conclusions and Recommendations** – Provides a summary and conclusions drawn from the results and interpretations. Recommendations are provided to improve quality for future investigations
- **Section 7.0, References** – Provides a listing of references cited in the report.

2.0 BACKGROUND

The Hanford Site is a 567 square mile area of semiarid scrubland covering the western part of the Pasco Basin in south-central Washington State. The site has 177 underground storage tanks, storing approximately 57 million gallons of liquid waste; the tanks are organized in 12 tank farms. Additionally, aboveground and underground facilities surround the tank farms to support waste disposal or retrieval operations.

A 3D electrical resistivity survey conducted near the southwest corner of the C tank farm. The C tank farm is located in the east central portion of 200 East Area of the Hanford Site (Figure 2-1), within Waste Management Area C.

The C tank farm area consists of the following facilities, shown graphically in Figure 2-2:

- Twelve 100-Series SSTs with a 530,000-gallon (2,000,000-liter) capacity
- Four 200-Series SSTs with a 55,000-gallon (210,000-liter) capacity
- 244-CR vault
- Eight diversion boxes
- Waste transfer lines
- Leak detection systems
- Tank ancillary equipment.

Specifically, the geophysical investigation was centered on UPR-200-E-86 (UPR-86), outside the tank farm fence (Figure 2-3). The UPR-86 is adjacent to UPR-81, which was imaged during 2009 using the same geophysical technique of acquisition and processing described in this report.

Figure 2-1. Location Map of Waste Management Area C in the 200 East Area of the Hanford Site.

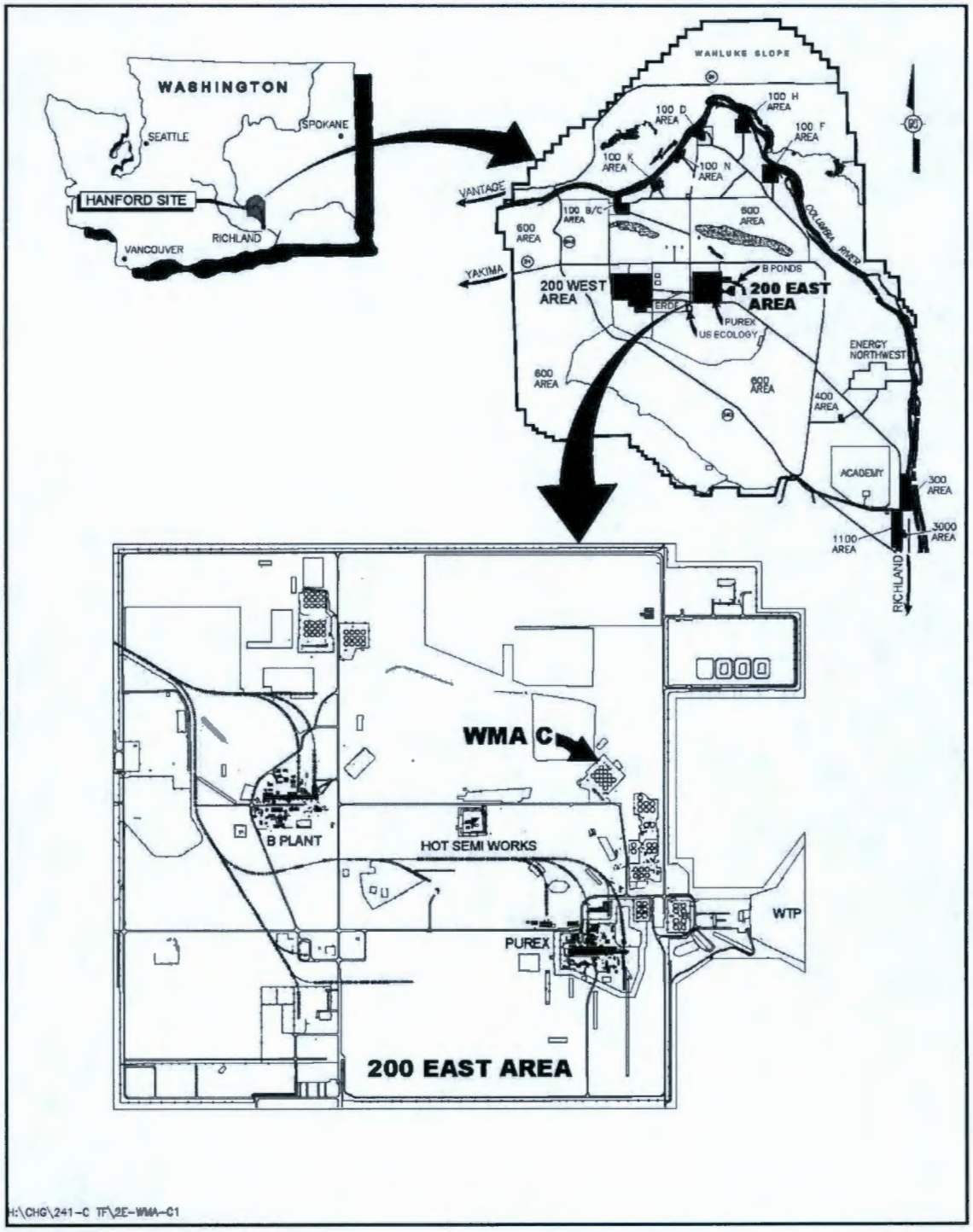

Figure 2-2. Map of the C Tank Farm and Surrounding Facilities.

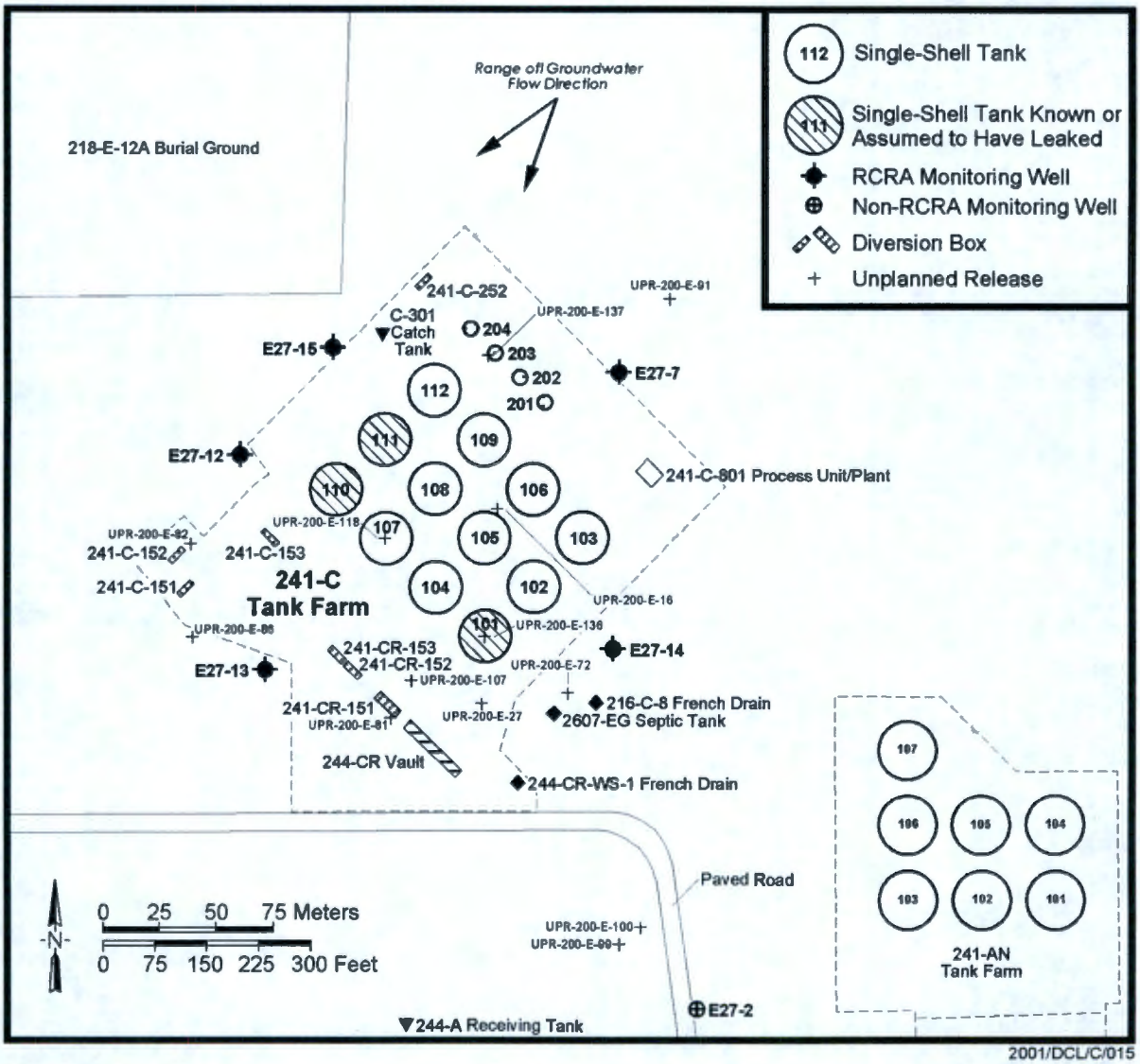

Figure 2-3. Map of the C Tank Farm and Surrounding Facilities.

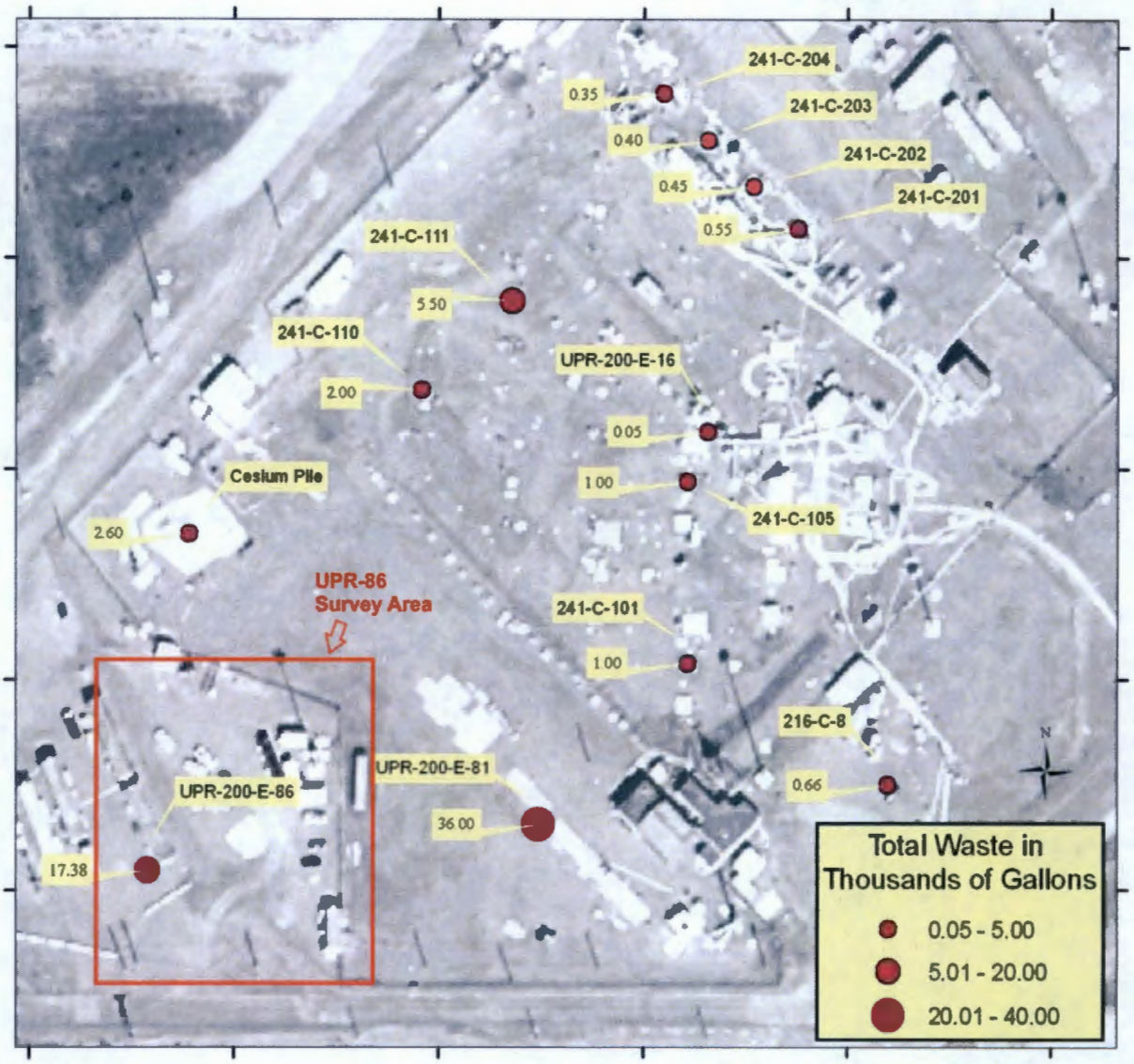

2.1 TANK FARM FACILITIES AND INFRASTRUCTURE

Tank farm construction at C farm occurred during 1943 and 1944, and the tanks were put into service in 1946. C farm is currently out of service pending final waste retrieval actions. The farm received waste generated by four major Hanford Site chemical processing operations: bismuth phosphate fuel processing, uranium recovery, plutonium-uranium extraction fuel processing, and fission product recovery (RPP-14430, *Subsurface Conditions Description of the C and A-AX Waste Management Areas*).

In addition to the tanks, the 244-CR vault exists to the south of the tanks. The vault is a two-level, multi-cell, reinforced concrete structure constructed below grade. It was constructed in 1946 and ceased operating in 1988. It was used to transfer waste solutions from processing and decontamination operations (DOE/RL-92-04, *PUREX Aggregate Area Management Study Report [AAMSR]*). The vault contains four underground tanks along with overhead piping and equipment. The two larger tanks, 244-CR-001 and 244-CR-011, have a capacity of 45,000 gallons (170,343 liters) each. The two smaller tanks, 244-CR-002 and 244-CR-003, have capacities of 14,700 gallons (55,494 liters) each (DOE/ORP-2003-11, *Preliminary Performance Assessment for Waste Management Area C at the Hanford Site, Washington*).

C farm also includes eight inactive diversion boxes along with the transfer pipes to the double-shell tank systems and associated equipment. Exterior water intrusion has been restricted from all diversion boxes used within the farms, and all boxes are currently inactive. The diversion boxes were an integral part of the waste transfer system (DOE/ORP-2003-11). Some boxes were the sites of contaminant releases to the subsurface, including the UPR around which this survey is focused. Other infrastructure systems in C farm include leak detection systems and tank ancillary equipment.

2.2 UNPLANNED RELEASES

Based on historical records, evidence exists that several UPRs occurred near the C tank farm. Figure 2-3 shows the location and estimated volumes of release for several UPRs in the vicinity of C farm. These releases have contaminated the soils within Waste Management Area C and are of interest to ongoing remedial field investigation/corrective measures study activities. The need to investigate UPR-86 was identified in RPP-PLAN-39114, *Phase 2 RCRA Facility Investigation/ Corrective Measures Study Work Plan for Waste Management Area C.*

On February 25, 1971, routine leak detection monitoring equipment detected a leak in the vicinity of transfer line 812. The line was being used to transfer process effluent waste (high-level plutonium-uranium extraction waste) from the 244-AR Vault to the C tank farm. The break occurred just south of diversion box 241-C-151 (RPP-35484, *Field Investigation Report for Waste Management Areas C and A-AX*). The volume and inventory of the leak was estimated to consist of approximately 17,385 gallons of waste containing 25,000 curies of cesium-137 (1.35 curies per gallon). According to RPP-RPT-42294, *Hanford Waste Management Area C Soil Contamination Inventory Estimates*, results of more recent studies based on vadose zone measurements accounted for only a fraction of the leak estimate based on these process records. Logging and sampling of holes placed at locations defined by the bounding surface occurrence of the leak showed levels of activity too low to be consistent with a release volume of 17,000 gallons.

2.3 SOIL SAMPLING AT UPR-86

Figure 2-4 shows the locations of 13 probehole locations around UPR-86 spill and 13 locations around CR-151 representing UPR-81. Several of these locations were geophysically logged with neutron probe for moisture and gamma. Soil samples for physical and geochemical characterization were extracted from a smaller percentage of probeholes, including C5952, C5952A, C5958, and C5960 at UPR-86 (PNNL-SA-60937) and C6392, C6394, C6400, C6402, C6404, and C6406 at UPR-81 (PNNL-SA-61511).

In general, both areas show isolated zones of high moisture in the upper 23 feet (7 meters), with up to 25 percent moisture by volume recorded by the neutron probe. These high moisture zones are typically less than 1-meter thick and likely represent fine-grained stringers embedded in a sandy gravel matrix of moisture values around 3 to 6 percent.

Figure 2-5 shows anion concentration data of sulfate and nitrate from the soil samples extracted from UPR-86 and UPR-81.

- Probehole C5960 in UPR-86 shows sulfate over 100 microgram/gram (ug/g) between 18 and 20 feet (5.5 to 6 meters) below ground surface (bgs) and at 82, 118 and 139 feet (25, 36, and 42.3 meters) bgs.
- Nitrate mass concentration data within all of UPR-86 region is quite low and ranged from non-detect to 21.4 ug/g (background is approximately 30 ug/g) (DOE/RL-92-24).
- To place these data in perspective, the average volume concentration for all of the samples at UPR-86 is 0.266 gram per liter (g/L) compared to BC Cribs concentrations of 250 g/L within the target zone (Rucker et al., 2009).
- No technetium-99 was detected in any samples associated with UPR-86.
- Uranium-238 was detected in a range between 0.263 ug/g to 1.47 ug/g for UPR-86 samples. This upper value of 1.47 ug/g is equal to 0.49 pCi/g of uranium-238 for UPR-86 samples.. Background value of uranium-238 is 1.39 pCi/g. Cesium-137 was not detected in any sample at UPR-86.

Figure 2-4. Probehole sampling at UPR-81 and UPR-86

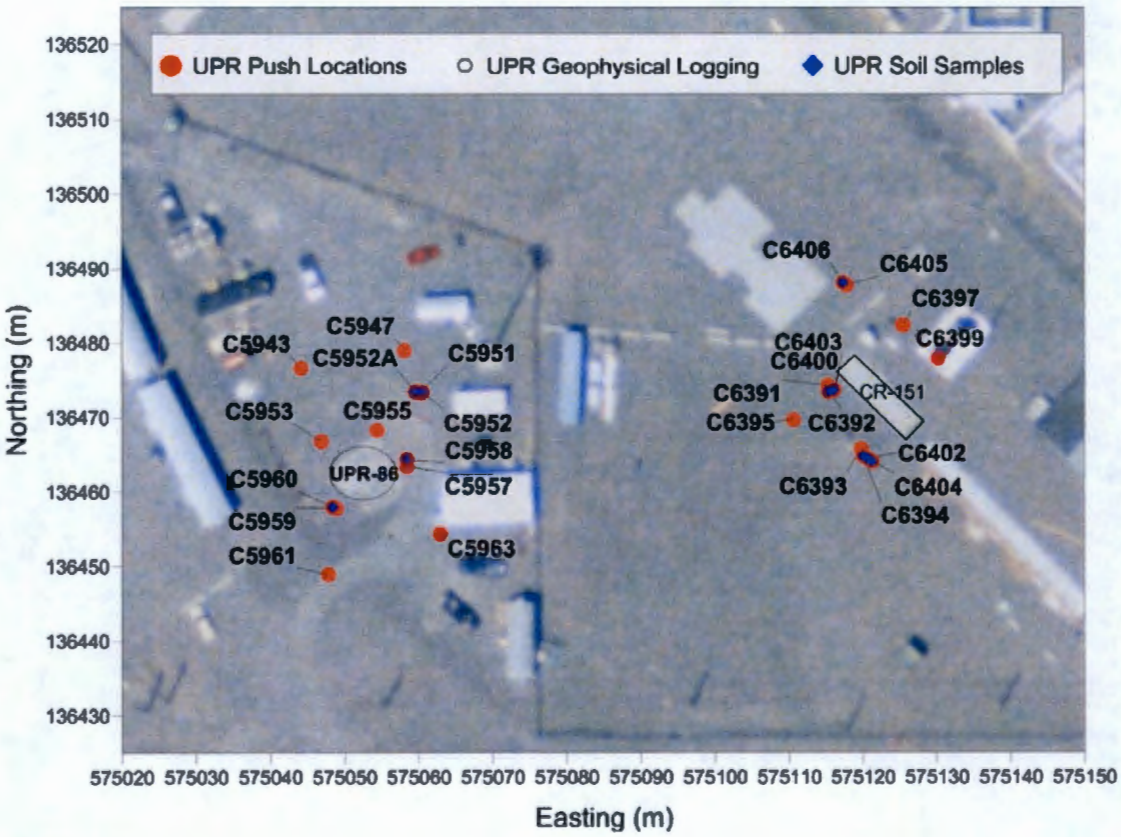

Figure 2-5. Sulfate and Nitrate Mass Concentrations for UPR-81 and UPR-86

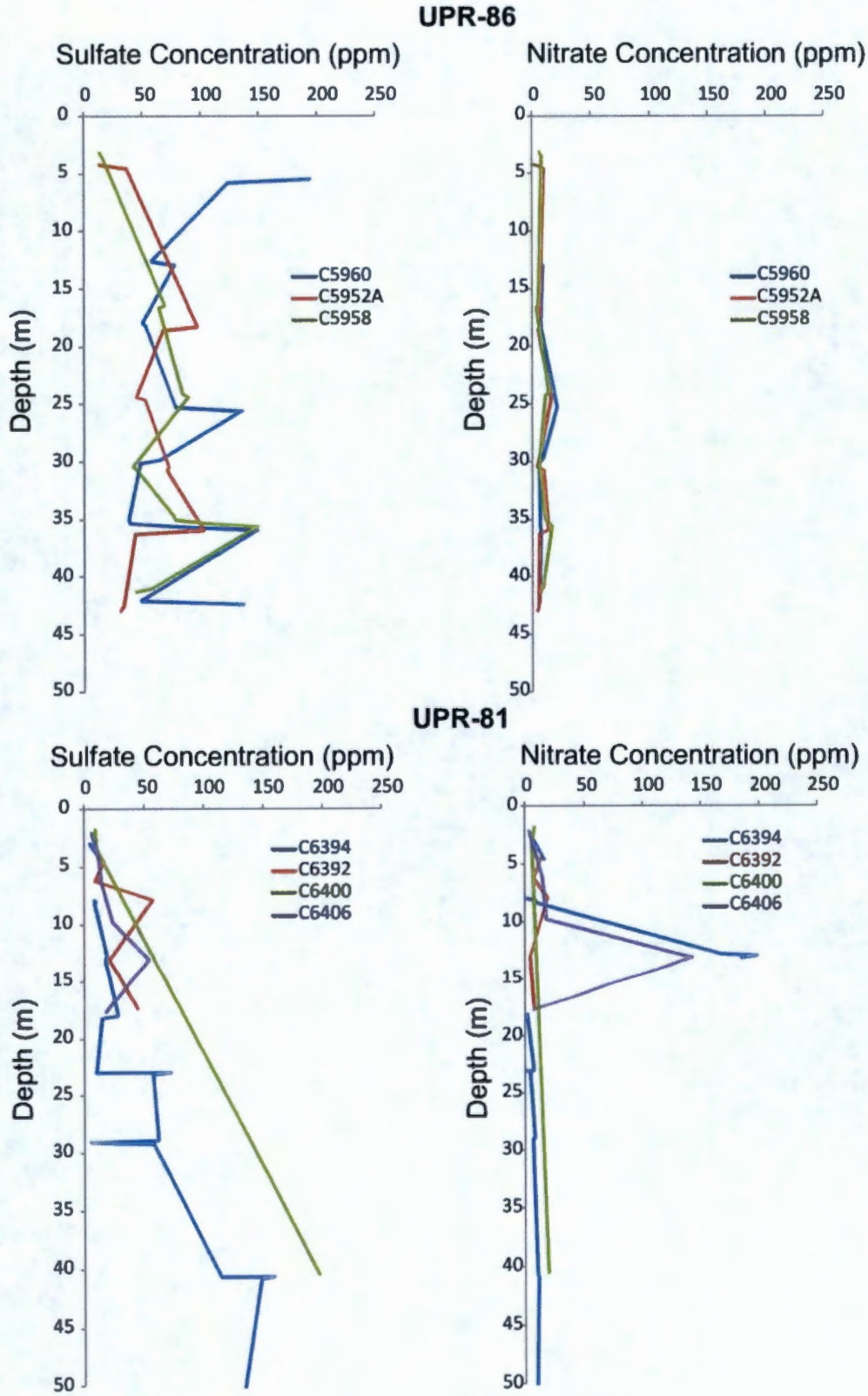

Probeholes associated with UPR-81 region for sulfate ranged from 6.7 ug/g to 198 ug/g (Figure 2-5).

- The highest sulfate concentration is associated with probehole C6400 at a depth between 132 and 135 feet (40.2 to 41.2 meters) bgs.
- Probehole C6394 had the next highest concentrations of sulfate at depths of 76 feet (23.2 meters), between 133 and 135 feet (40.8 to 41.2 meters), and at 170 feet (51.8 meters) bgs that exceeded 100 ug/g. Nitrate concentrations ranged from non-detect to 199 ug/g. The highest nitrate concentrations are associated with this probehole as shown in Figure 2-5 between a depth of 42 to 44 feet (12.8 to 13.4 meters) bgs.
- Technetium-99 was detected in two samples associated with UPR-81. These samples were from C6392 at depths of 14 to 15 feet (4.25 meters) and 19.5 to 21.5 feet (6 meters). The technetium-99 concentration values were 1.4E-03 ug/g or 23.7 pCi/g and 2.66E-03 ug/g or 45.1 pCi/g respectively. Uranium-238 was detected in a range between non-detected to 1.01 ug/g. This upper value of 1.01 ug/g is equal to 0.34 pCi/g of uranium-238. Background value of uranium-238 is 1.39 pCi/g. Cesium-137 ranged from non-detect to 7.31×10^{-5} uCi/g sample at UPR-81.

3.0 QUALITY ASSURANCE

Collection and analysis of SGE data are performed under a project-specific quality assurance plan using a graded approach that conforms to applicable requirements from Columbia Energy and Environmental Services, Inc. quality assurance procedures (CEES-0333, *Quality Assurance Plan for Surface Geophysical Exploration Projects*). These procedures implement the requirements of ASME NQA-1, *Quality Assurance Requirements for Nuclear Facility Applications*, and DOE O 414.1C, *Quality Assurance*. Work not covered in the quality assurance plan will conform to accepted industry standards for SGE and sound engineering principles.

This quality assurance plan implements the criteria of DOE O 414.1C and the following requirements from ASME NQA-1:

- Organization (Requirement 1)
- Quality Assurance Program (Requirement 2)
- Instructions, Procedures, and Drawings (Requirement 5)
- Document Control (Requirement 6)
- Corrective Action (Requirement 16)
- Quality Assurance Records (Requirement 17).

Columbia Energy and Environmental Services, Inc. and hydroGEOPHYSICS, Inc. collect data using designed systems or off-the-shelf commercially available hardware. Designed systems conform to applicable requirements in approved procedures that address design, design analysis, design verification, and engineering drawing.

A project specific software management plan, CEES-0338, *Software Management Plan for Surface Geophysical Exploration Projects*, was prepared to implement a graded approach to software management in accordance with the following requirements documents:

- ASME NQA-1, Subpart 2.7, "Quality Assurance Requirements for Computer Software for Nuclear Facility Applications"
- CEES-0333
- CE-ES-3.5, *Software Engineering*
- Contract 28090, *High Resolution Resistivity Characterization of Single Shell Tank Farm Waste Management Areas*
- DOE O 414.1C.

3.1 CALIBRATION AND MAINTENANCE OF EQUIPMENT AND INSTRUMENTS

Calibration and maintenance of equipment used for data collection is addressed in CEES-0360, *Surface Geophysical Exploration System Design Description*. Where periodic calibration and/or maintenance of instruments used to collect quality affecting data is recommended, those

instruments were current on calibration at the time the instrument was used for data collection and the calibration certificate is maintained in the project files.

Field notes are used to document the specific instruments used. Electronic logs are utilized to provide traceable documentation for each data set collected. Information recorded in the electronic field log includes date, instrument identification, operator, and applicable settings for each data set collected. All instruments have current calibration certificates, and documentation is maintained in the project files. Instrument calibration frequency and calibration tests performed in the field are documented in the system design description (CEES-0360).

3.2 DATA COLLECTION

The setup, operation, and maintenance of the SGE equipment used in collecting and analyzing resistivity data is described in CEES-0360. This document identifies the requirements for the hardware and software used for data collection and analysis and provides a rationale for the hardware and software selected for use.

Calibration requirements are described for hardware used to collect geophysical data. As an example, Advanced Geosciences, Inc. (AGI), the manufacturer of the resistivity data acquisition instrument (SuperSting R8®) recommends a yearly calibration of internal calibration resistors. The calibration is performed at the manufacturer's facility and a certificate of calibration is provided. A copy of the calibration documentation, serial numbers, and expiration dates are maintained in project files.

In addition, daily inspection of the receiver calibration is performed onsite using the manufacturer-supplied calibration resistor test box. The supplied test box is connected to the SuperSting R8 before commencing the daily survey. A specific calibration test firmware is provided within the SuperSting and provides the operator with a pass/fail indication for each of the eight receiver channels. If any of the channels fail, a recalibration or repair is required.

In addition to calibration checks, data accuracy was evaluated by performing reciprocal data collection for the UPR-200-E86 project. Reciprocal collection was used as a tool to assure the electrical resistivity data are accurate and repeatable. The transfer, storage, and management of data collected in the field are described in the system design description (CEES-0360).

3.3 ELECTRICAL INTERFERENCE MONITORING

Electrical interference can affect resistivity measurements in two ways:

1. Grounded conductive infrastructure (pipes, tanks, fences) may provide a preferential current pathway that distorts predictable current flow paths within the earth
2. Electrical noise (voltage/current) sources from electrical systems (cathodic protection, pumps, motors, earth grounding arrays, etc.) may inject a competing signal. Electrical noise interference can be minimized by identifying noise sources and then turning off electrical sources where possible for the duration of the resistivity surveying.

® SuperSting R8 is a registered trademark of Advanced Geosciences, Inc.

A passive monitoring system was used to detect and map possible electrical noise interference prior to the start of resistivity measurements at UPR-86. The electrical interference survey consists of temporarily wiring several electrodes or steel-cased monitoring wells, distributed over a survey area, to a distribution panel. A digital recording oscilloscope is connected at the electrode measuring points (two at a time) and the background electrical field is digitally recorded via a laptop computer. The oscilloscope operates via the universal serial bus port on the laptop computer and does not transmit signal into the ground. Data are recorded before and after electrical systems are turned off to verify the reduction in electrical interference. The data are then assessed at an offsite location and recommendations to minimize electrical interference are made. The electrical interference survey is designed to identify the magnitude, frequency, and cycle time of possible interference. A suitable electrode distribution (an example for a tank farm survey is shown in Figure 3-1) may allow an assessment of the location and directionality of possible localized noise sources such as pumps and motors. The actual location and quantity of electrodes are determined as part of the project survey design. For this survey, the wells selected were used as sampling points for the electrical interference testing.

Figure 3-1. Example of Electrical Interference Monitoring.

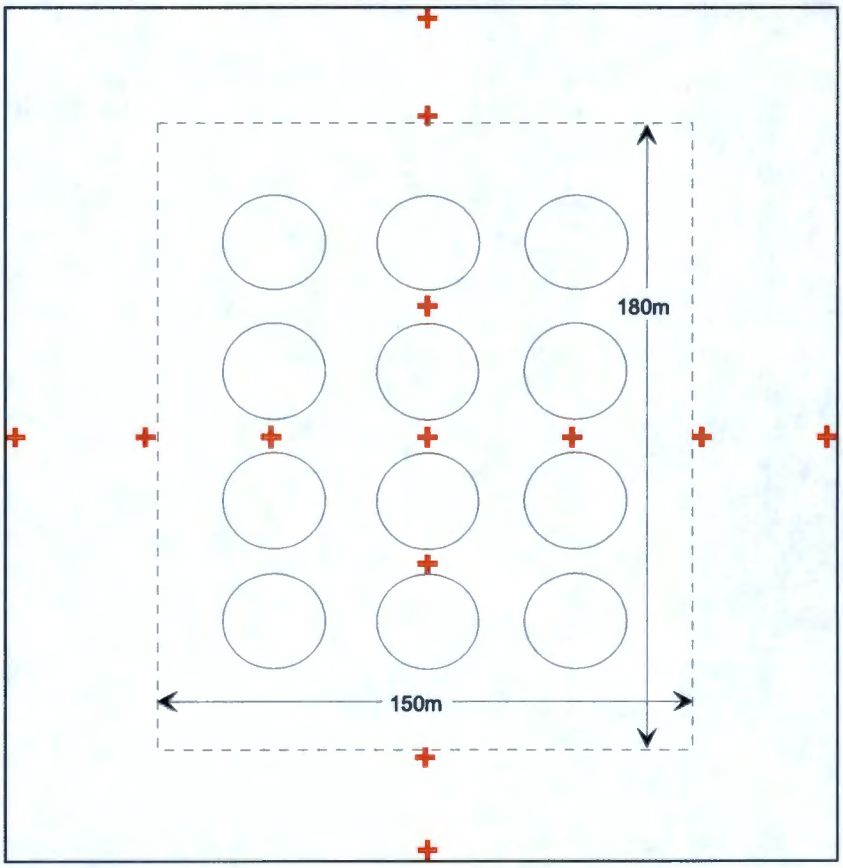

Note: Electrode arrangement for a generalized tank farm, electrodes are shown as red +.

3.4 EQUIPMENT TESTING

3.4.1 SuperSting

Daily inspection of the receiver calibration was performed onsite using the manufacturer-supplied calibration resistor test box. The supplied test box is connected to the SuperSting R8 before commencing the daily survey. A specific calibration test firmware is provided within the SuperSting and provides the operator with a pass/fail indication for each of the eight receiver channels. If any of the channels fail, a recalibration or repair is required.

3.4.2 Switchboxes

A relay test was performed on a daily basis. For the relay test, the operator connects a switchbox or switchboxes to the SuperSting R8 and performs the relay test that is incorporated into the SuperSting R8 firmware. This test sends a signal to each switchbox electrode to assess the functionality of the relays on each switchbox electrode channel. The SuperSting reports the success or failure of each relay (switchbox electrode channel) as a pass or fail. The relay test only inspects the operability of each relay.

As part of field equipment testing on all resistivity surface exploration geophysics deployments at the Hanford Site, it is necessary to provide equipment evaluation specifically with regard to the functionality of the AGI SuperSting R8 Resistivity meter ("Sting") electrode multiplexors (switchboxes). The switchboxes come in three standard capacities, all in increments of 28 switches, e.g., 28, 56, and 84 switches. Any combination of these switchboxes may be used on a Hanford Site deployment of SGE.

A Switchbox test was performed on all switchboxes used on a weekly, and as needed basis. For the Switchbox test, the operator connects a switchbox to the SuperSting R8 and to a switchbox diagnostic tester (SBDT) (hydroGEOPHYSICS, Inc, Tucson, Arizona). The SBDT simulates an actual resistivity survey using a network of resistors of known resistance. The measured data are compared to the known resistances for the SBDT, and success or failure is reported for each switchbox electrode channel as a pass or fail. The switchbox test evaluates the operability of each relay and, in addition, evaluates any possible shorting, lack of isolation or failures of internal electronics that control the relays. If a relay fails in the opened or closed state during typical testing, relatively high measurement errors, sometimes exceeding 100 percent relative to the standard baseline results recorded for the SBDT by the High Resolution Resistivity® Leak Detection and Monitoring® Data Acquisition System, can be expected.

The selection of an appropriate error threshold for passing or failing needs to be consistent with the type of survey being performed and environmental conditions that could be encountered during testing. A 5 percent error threshold is typical for industry use in bench-scale testing of equipment, and this level could be very appropriate for some applications. Under a bench testing setting, where environmental conditions are generally controlled, experience has shown that recorded Sting measurements for operational relays within a switchbox can be much less than

® High Resolution Resistivity (HRR) and Leak Detection and Monitoring (LDM) are trademarks of hydroGEOPHYSICS, Inc., Tucson, Arizona.

5 percent of standard baseline values for the SBDT. The 5 percent level is also supported by the manufacturer, AGI in bench-scale evaluation of switchbox relays in their facilities.

However, under field conditions, where changes in ambient temperature, wind conditions, and electrical interference can potentially affect measurement error during data acquisition, it is possible that this 5 percent pass/fail threshold may not be adequate and could potentially result in apparent relay failures in a fully operational switchbox. Geophysical resistivity data taken in less than ideal environment conditions can often exceed a 5 percent error in repeatability, but can still be used to produce usable results. Therefore, to account the additional effects of field conditions, professional judgment is that a 10 percent threshold would be a more appropriate level to use, and this level was initially used in switchbox testing for this project. As additional experience is gained with SBDT field testing, this value will be reevaluated as an effective pass/fail threshold.

3.5 DATA PROCESSING

The process used to filter the raw data is described in the system design description (CEES-0360). Data are downloaded from the resistivity instrument and parsed into a usable format. Data filtering techniques are then used to remove data spikes or anomalous data caused by data acquisition card instabilities, or extraneous current sources.

Data filtering is performed by copying the parsed raw data into an Excel® data filtering template that contains a series of graphs that show the various data parameters. The process of filtering eliminates data points, but no data modification (rounding, averaging, smoothing, or splining) is permitted. The rationale is to seek out and remove spurious points that do not conform to the data population or points that violate potential theory.

The final step is to inverse model the measured data to obtain the spatio-temporal distribution of electrical resistivity. Inverse modeling is accomplished using either EarthImager3DCL® (EI3DCL) or RES3DINVx64 (RES3D). Verification and testing of the inversion software was performed and documented in RPP-RPT-35104, *Verification and Testing of the EarthImager Series of Electrical Resistivity Inversion Codes – A Benchmark Comparison*. Verification and testing was performed on the existing two-dimensional (2D) and 3D versions of the software as well as the upgraded 64-bit, multi-threaded versions developed for tank farm projects.

The objective of the verification and testing study was to demonstrate that the resistivity inversion codes were comparable to known conditions from a pilot-scale field resistivity experiment. The pilot-scale field experiment was used to test the well-to-well inversion methodology by establishing a known conductive target in the subsurface and making measurements with a set of 27 simulated wells. To date, there is no industry standard for the well-to-well resistivity imaging technique, which necessitated the field experiment. The field experiment was designed to test both inversion code's ability to replicate a target of known geometry. The subsurface geophysical target was an amended, electrically conductive soil, buried approximately 1.6 feet (0.5 meters) bgs. The 27 wells were distributed around the target in a pattern similar to tank B-105 in the B tank farm.

® Excel is a registered trademark of the Microsoft Corporation.
® EarthImager3DCL is a registered trademark of Advanced Geosciences, Inc.

From the above descriptions, it is obvious that data processing is performed using a number of software packages. The requirements and responsibilities for the identification, evaluation, development, testing, and maintenance of quality-affecting software acquired, developed, or modified in support of the SGE efforts are defined in the CEES-0338.

4.0 DATA ACQUISITION AND PROCESSING METHODOLOGY

Data acquisition for a 3D electrical resistivity survey at the UPR-86 site began on March 17, 2010, and was completed on March 21, 2010. The geophysical survey was initiated to collect data on both surface electrodes and electrodes buried deeply beneath the surface (i.e., depth electrodes). The 3D methodology is in contrast to most previous SGE surveys, where data acquisition was relegated to sets of parallel and orthogonal 2D profiles collected along individual lines, which when grouped together produce a 3D image. A 3D survey is superior to a 2D survey because much more data are collected to define the electrical properties of the subsurface. However, 3D surveys usually take much longer to acquire and require more resistivity equipment.

The amount of infrastructure at the site, shown in Figure 4-1, necessitated the 3D acquisition methodology. The infrastructure within and surrounding the project area is assumed to act as a 3D network of pathways for electrical current in the ground that would channel electrical currents laterally away from 2D survey lines. Producing a reasonable model domain from 2D collected data relies on the assumption that target geometry beneath each 2D measured line does not significantly channel electrical currents away from each 2D line in a lateral direction. Reference the following documents:

- Yang and Lagmanson 2006, Comparison of 2D and 3D Electrical Resistivity Imaging Methods, Symposium on the Application of Geophysics to Engineering and Environmental Problems
- Gharibi and Bentley 2005, "Resolution of 3-D Electrical Resistivity Images from Inversions of 2-D Orthogonal Lines").

The abundance of infrastructure within the project area violates this assumption and is likely to cause a disturbance known as a "3D effect." The 3D survey utilized in this study aims to minimize this disturbance.

Data collection activities, along with the basis and selection of data collection equipment, and data processing are described in the following sections.

4.1 SURVEY DESIGN

Resistivity data were collected based on a 3D data acquisition method that made use of both surface and depth electrodes. The surface electrodes were distributed across a uniform grid to optimize the inversion models used in the data analysis and interpretation. The significantly larger amounts of data associated with a 3D survey, relative to a 2D survey, makes an optimized geometry crucial to reduce modeling run times and analysis. For the UPR-86 survey, 301 surface electrodes were distributed across a site 66 meters by 78 meters, with electrodes spaced nominally every 3 meters in the east-west direction and nominally every 6 meters in the north-south direction. Some positions along this grid were skipped based on the proximity to near surface infrastructure or surface obstructions.

Further resolution is possible by adding depth electrodes to a surface electrode geometry, whereby electrical current and voltage measurements can be made near or within a target. Depth electrodes

have the added benefit of being further from near-surface infrastructure and associated electrical interference and noise. For the UPR-86 survey, five depth electrodes labeled C-5943, C-5947, C-5957, C-5959 and C-5963 were placed opportunistically, that is, in areas devoid of surface infrastructure. The footprint of the depth electrodes did not necessarily align to the surface grid. Table 4-1 displays the locations and depths associated with each depth electrode.

Figure 4-1. Electrode Layout and the Local Distribution of Infrastructure for the UPR-200-E-86 Survey Area.

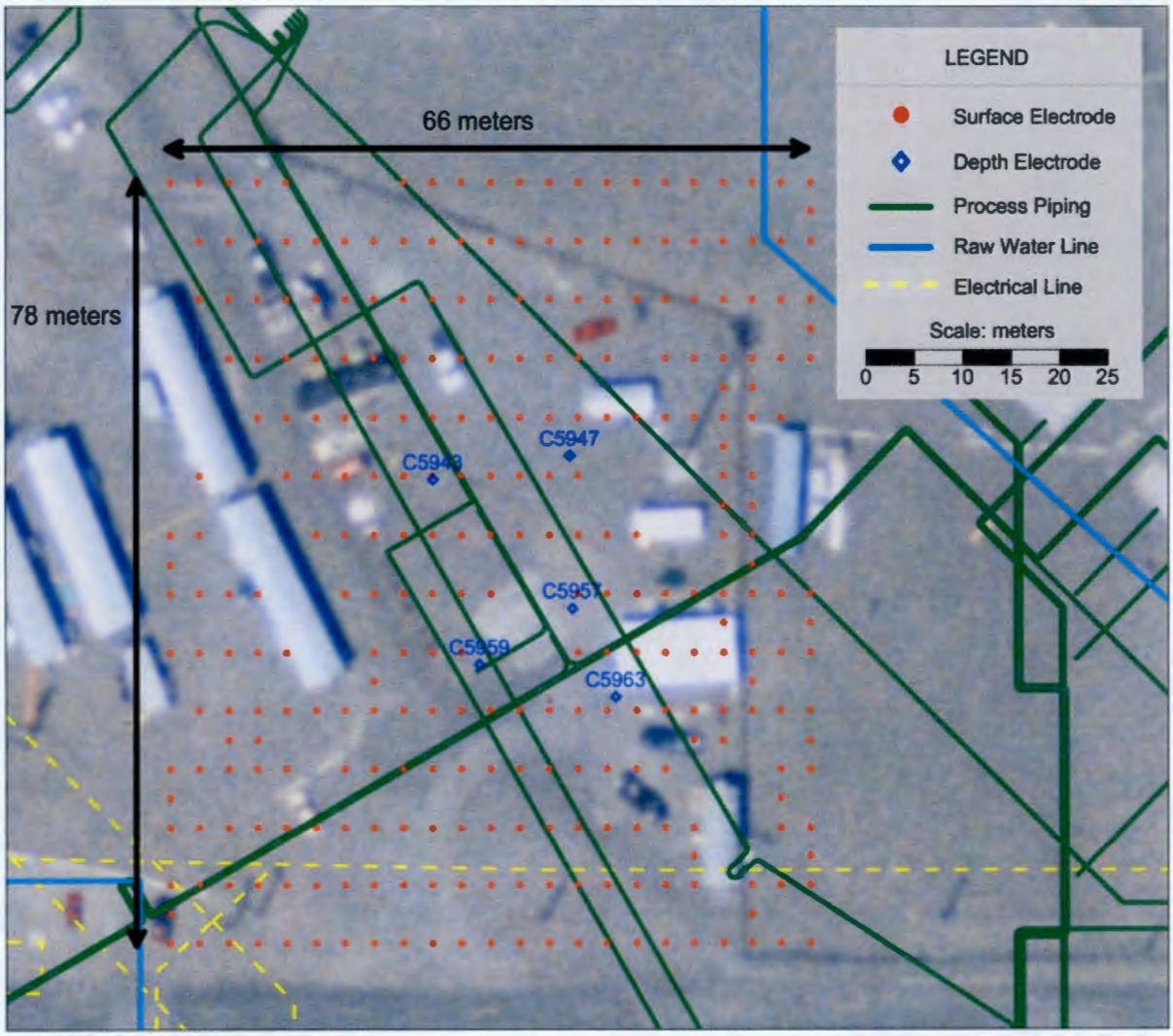

North is located at the top of the figure.

Table 4-1. Subsurface (Depth) Electrodes Placed around UPR-200-E-86.

Probehole Number	Surface Elevation (meter)	Northing (meter)	Easting (meter)	Electrode Depth (meter)	Electrode Depth (feet)
C5943	205.4	136476.6	575044.1	27	89
C5947	204.99	136479.0	575058.1	46	151
C5957	205.66	136463.5	575058.4	44	144
C5959	205.85	136457.8	575048.9	29	95
C5963	205.65	136454.4	575062.9	29	95

4.2 EQUIPMENT

4.2.1 ELECTRODE AND CABLE LAYOUT

The first stage of the project was to assemble all available infrastructure maps for the C farm area of investigation. The resulting maps were combined into an AutoCAD® drawing and subsequently used to define the coordinates for electrode placement. The maps containing infrastructure locations, including subsurface pipes/structures and surface structures, were digitized and combined with the electrode locations. Electrode locations were then modified to avoid being directly over infrastructure where possible. Movements of electrodes were limited by maintaining a uniform 3 meter grid layout to support data processing software. The final electrode layout was then uploaded into a Leica 1200 Global Positioning System which was used to mark locations on the ground surface. The Leica system has subcentimeter accuracy, assuring the survey geometry will remain intact.

The electrodes are connected to the resistivity acquisition meter by way of multi-cored cables and multiplexors. For the UPR-86 project, a total of four cables were deployed, with each cable allowing up to 84 electrodes at a 3-meter spacing. The cables were placed in a serpentine pattern with cable offset of 6 meters in the north-south direction. In some areas, the specific location of the cable was modified to accommodate the infrastructure and barriers.

Six (AGI-manufactured) 56-electrode switch boxes (multiplexors) acted as junction boxes to connect the resistivity meter to the ground cables. The multiplexors provided a 336 electrode capability, of which 301 were used for surface electrodes and five for depth electrodes. A separate patch panel was used to connect the depth electrodes to the multiplexor. Figure 4-2 shows an example layout of the resistivity gear.

® AutoCAD is a registered trademark of AutoDesk, Inc.

Figure 4-2. Resistivity Data Acquisition System.

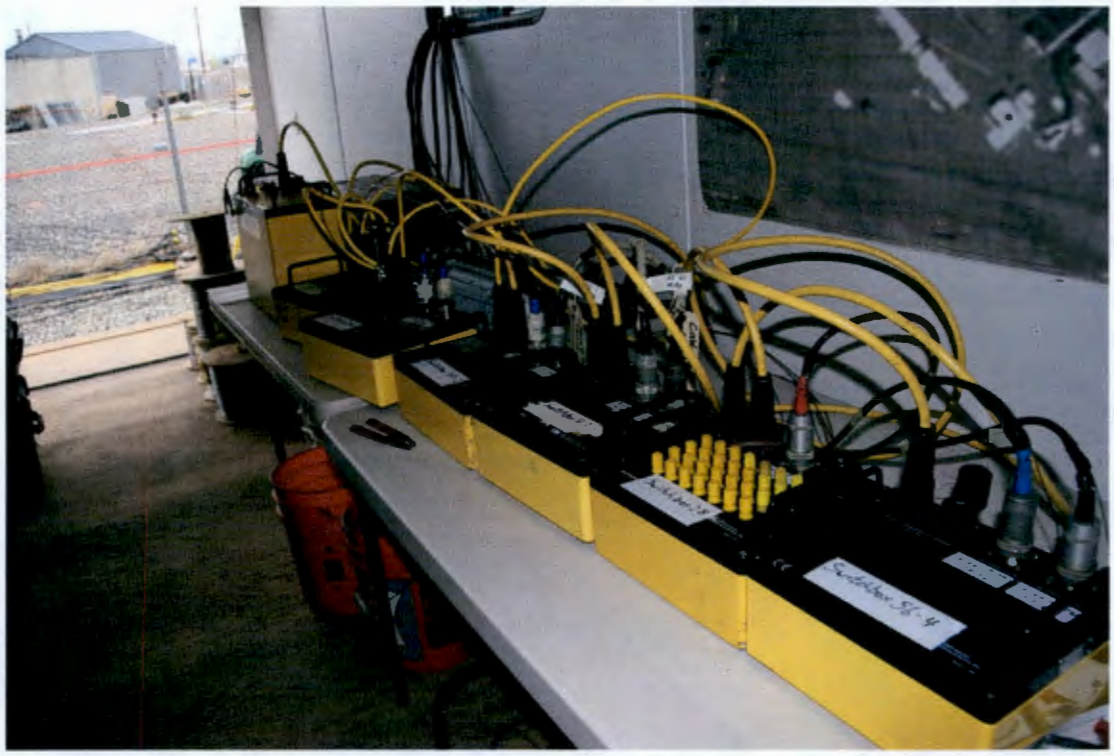

4.2.2 RESISTIVITY METER

The AGI-manufactured (SuperSting R8®) resistivity meter, was used for resistivity data acquisition. The meter is capable of full 8-channel acquisition, whereby 8 simultaneous measurements of voltage can be made during electrical current transmission. The R8 meter has been used for many SGE projects and has proven itself to be reliable for long-term, continuous acquisition campaigns.

Intensive quality assurance was completed before and after the survey to ensure the equipment was functioning appropriately as well as the quality of data was acceptable. Calibration requirements are described for hardware used to collect geophysical data in CEES-0360. As an example, AGI recommends a yearly calibration of internal calibration resistors. The calibration is performed at AGI's facility and a certificate of calibration is provided. A copy of the calibration documentation, serial numbers, and expiration dates are maintained in project files.

Daily inspection of the receiver calibration was also performed onsite using the manufacturer-supplied calibration resistor test box. The supplied test box is connected to the SuperSting R8 before commencing the daily survey. A specific calibration test firmware is provided within the SuperSting and provides the operator with a pass/fail indication for each of the eight receiver channels. If any of the channels fail, a recalibration or repair is required.

® SuperSting R8 is a registered trademark of Advanced Geosciences, Inc.

4.3 ACQUISITION METHODOLOGY

The resistivity acquisition included a pole-pole array, where one electrode from each of the transmitting and receiving electrode pairs were placed effectively at infinity. Practically, these poles are placed remotely, anywhere from 2 to 5 times the maximum internal electrode distance away from the site in opposite directions. The remote electrodes from the UPR-81 survey were reoccupied for the UPR-86 survey.

Data collection was initialized on March 17, 2010, and completed March 21, 2010, with approximately 80 hours of near-continuous acquisition. Operations were interrupted briefly to perform the daily inspection of the resistivity meter. Data were collected around the clock, 24 hours a day over a long weekend to minimize impacts to tank farm operations. Additionally, continuous data collection was used to minimize the influence of changing moisture conditions over longer periods of time. Personnel were maintained onsite at all times to monitor data collection and to keep the cable area clear of vehicles and equipment that could damage equipment and impact data quality.

Both forward and reverse data sets were collected during data acquisition in order to increase the resolution of the resistivity survey and evaluate data quality. Forward and reverse measurements are acquired by switching the transmitting and receiving electrodes to produce a reciprocal dataset. The two sets of data ensured that each electrode acted as both transmitter and receiver; both are needed for quality control. The theory of reciprocity implies that a homogeneous earth should allow for consistent measurements in both forward and reverse measurement conditions. Thus, by varying selected reciprocal percent difference thresholds, the ratio between data quality and quantity can be assessed. For this survey effort, data measurements with a relative percent difference greater than 5 percent were considered unacceptable and removed from the dataset before numerical inverse modeling.

4.4 DATA PROCESSING

4.4.1 Data Reduction

All raw data collected at the C farm UPR-86 site were compiled into a relational database. Raw data included both electrical resistivity data and Global Positioning System positional data to geo-reference the resistivity data. A set of queries was designed to segregate reciprocal pair data points and assign each data point distinguishing characteristics not retained in the raw sting file. This information included electrode type and a sequential electrode number (as designated in the survey design). Additional data fields were added for the calculated distance between electrodes and percent error between reciprocal data. The data were then exported from the database for graphical filtering and plotting in a spreadsheet.

Four important diagnostic data parameters from the raw data include voltage/current (V/I; resistance), repeat error, reciprocal error, and electrical current output. The repeat error is a calculated percent error between cycled/repeated measurements. A plot of these data can provide information with regards to the statistical variation of the data population.

The process of data editing identifies and eliminates data points, but no data modification (rounding, averaging, smoothing, or splining) is permitted. The rationale is to seek out and

remove spurious points that do not conform to the data population or points that violate potential theory. The first step in this editing process was to remove data outside of the statistical population – negative V/I, noise, high instrument error, low current, low voltage, etc. Figure 4-3 shows the raw data distribution of the forward and reverse data, while Figure 4-4 shows the same datasets after filtering. The next step in data reduction was to apply a data quality filter based on reciprocity. All data with a reciprocal percent difference greater than 5 percent was removed.

Figure 4-3. Forward and Reverse Data Sets (Raw Data).

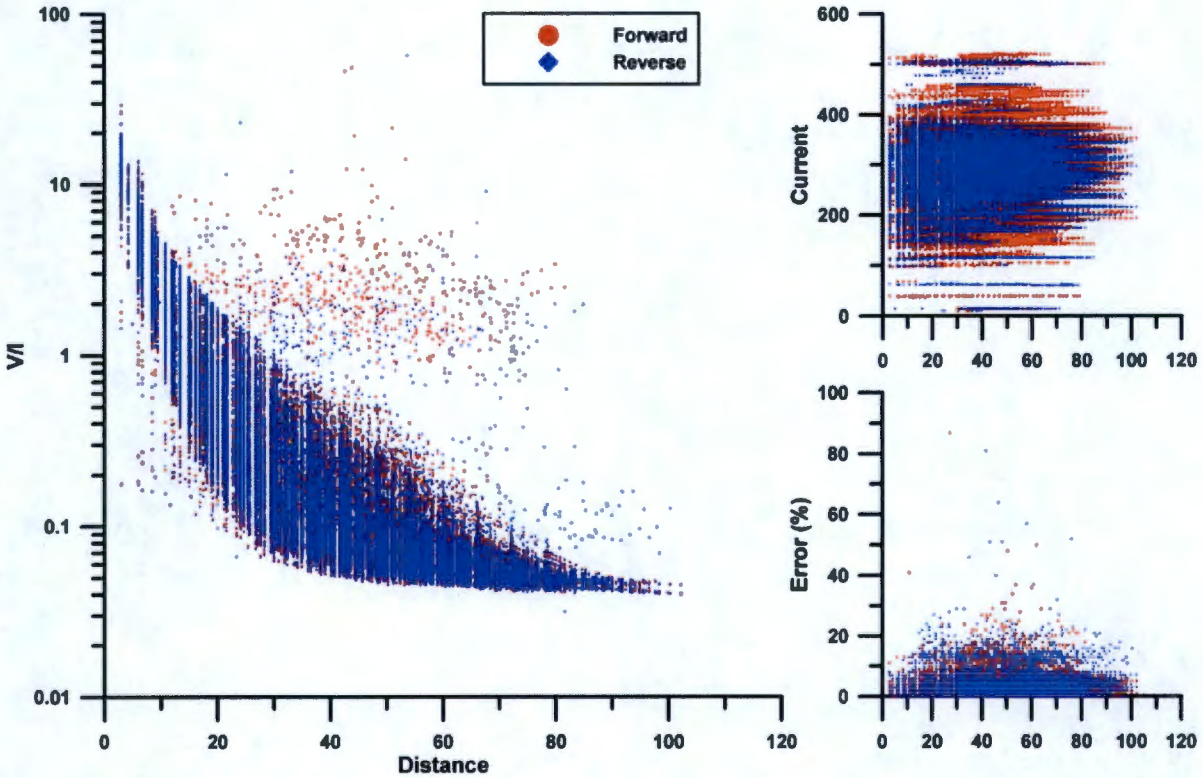

Raw data distribution for (1) V/I, resistance (left), (2) Error, and (3) Current (lower right). All are plotted against the distance between transmitting/receiving electrode pairs.

Figure 4-4. Forward and Reverse Data Sets after Data Editing.

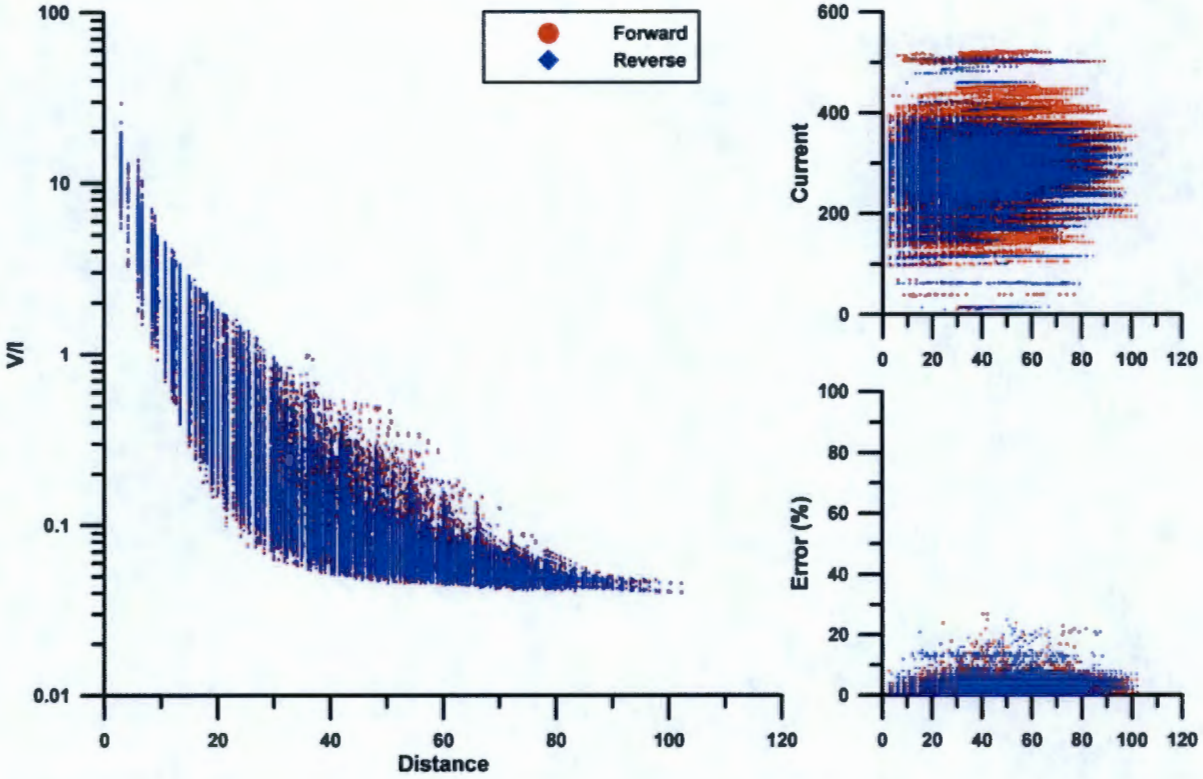

Data distribution after editing for (1) V/I, resistance (left), (2) Error, and (3) Current (lower right). All are plotted against the distance between transmitting/receiving electrode pairs.

Table 4-2 displays the percentages of data removed or retained during steps of the editing process.

Table 4-2. Number of Data Points Retained During Data Editing Steps.

	Forward	Reverse	Sum	Percent of Total
Total Raw	47,879	47,348	95,227	100.0
Total Combined Reciprocal	44,456	44,456	88,912	93.4
Total Edited	37,939	37,939	75,878	79.7

4.4.2 Depth Electrode Data Analysis

To evaluate the quality of depth electrode data, histograms showing V/I, electrical current, and error were plotted to assess performance (Figure 4-5). Based on this analysis, it was determined that depth electrode C-5947 does not fit the overall population based on both the repeat error

distribution and electrical current. The electrical current output is generally less than 20 milliamps (mA), where most others average around 280 mA. The performance could be due to a bad completion, resulting in poor electrode contact reducing the transmission of current. Including poor quality data in an inversion model will contribute to unsatisfactory model results. Therefore, data associated with C-5947, including depth-to-depth and depth-to-surface combinations were removed from the overall dataset.

Figure 4-5. Depth Electrode Histogram Analysis for UPR-E-86 Showing Analysis of (A) V/I Data, (B) Current Values, and (C) Error Values.

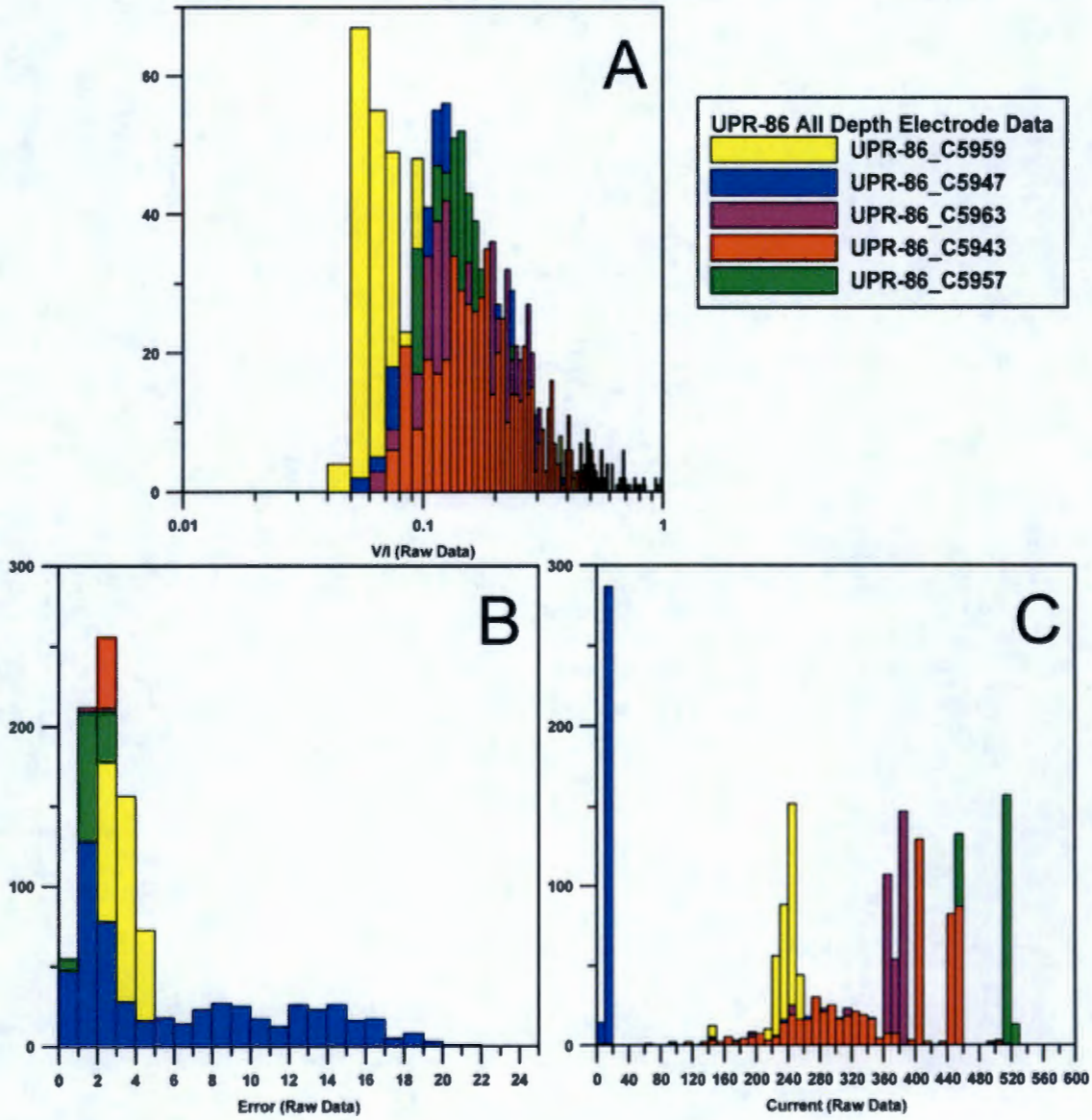

V/I = resistance

4.4.3 3D Inverse Modeling

Popular use of the RES3D series of resistivity inversion codes has led both professional and academic users to regard these codes as industry standard software. The UPR-86 modeling effort used RES3DINVx64, a 64-bit multi-threaded version developed specifically for a large number of electrodes.

In general, inverse modeling can be summarized in the following five steps. These steps are also shown graphically in a flowchart provided in Figure 4-6.

3. The study site's voltage data has been measured and is discretized into grid nodes using a finite difference or finite element mesh. The meshing parameters used in either case, to design the computational grids, are dependent on electrode spacing used in site-specific data acquisition.

4. The inversion will set out to estimate the true resistivity at every grid node. An initial estimate of the subsurface properties is made based on the literal translation of the pseudo-section to a true resistivity, a constant value, or some other distribution from *a-priori* information. A forward model run with these initial estimates is made to obtain the distribution of voltages in the subsurface. The root-mean-square (RMS) error is calculated between the measured voltage and the calculated voltage resulting from the forward run.

5. Based on the degree of model fit to field measurements, the initial estimate of resistivity is changed to improve the overall model fit and the forward model with the updated estimates is rerun. The iterative method linearizes a highly nonlinear problem using Newton's method. Using this method, the inverse modeling code essentially solves the linearized problem to obtain the change in modeled resistivity (Δm) for the next iteration.

6. The resistivity model is updated using the general formula $m_{i+1} = m_i + \Delta m$, where $_{mi+1}$ is the resistivity in a model cell at the next iteration, and m_i is the current value.

7. Steps 3 and 4 are repeated until the RMS error change between successive iterations reaches an acceptable level.

Figure 4-6. Flowchart of the Resistivity Inversion Process.

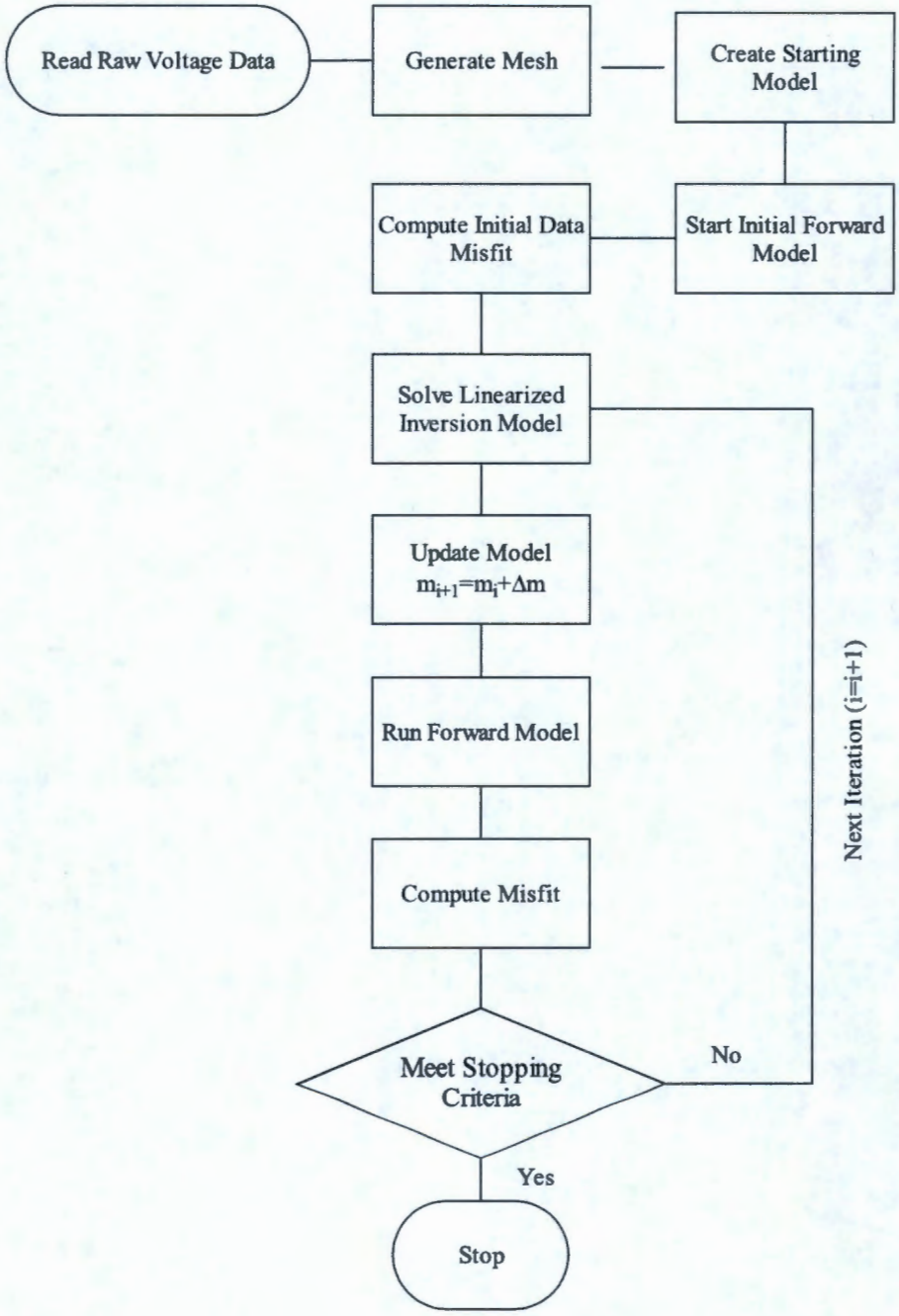

4.4.4 Inversion Model Parameters

Inversion software uses a series of user defined parameters to control the direction of the inversion modeling process. A description of the inversion parameters used with the RES3D inversion software package is provided in Section 4.3.3 of RPP-RPT-42844, *Reanalysis of Surface Geophysical Exploration Resistivity Data for the 241 T Tank Farm.*

5.0 RESULTS

Upon completion of data filtering, measured data from the UPR-86 site were inverse modeled using the RES3DINVx64 software package. For specific details of the SGE resistivity method and theoretical basis applied to inverse modeling, the reader is referred to discussions provided in Appendix A of RPP-34690, *Surface Geophysical Exploration of the B, BX, and BY Tank Farms at the Hanford Site.*

To accomplish the 3D inversion, every surface and depth electrode was geo-referenced (using the Washington State Plane – Meters coordinate system) to allow absolute placement of an electrode within the inversion algorithm. Although the survey area is flat, elevation data were also used to reflect the elevation differences between the surface and depth electrodes. After inversion, the final 3D inversion results were interpolated and visualized using the Rock Works™ visualization software package and Surfer® surface contouring package.

The initial scope of work for the C farm UPR-86 resistivity investigation was designed to perform a full inversion analysis of the 3D data that included the use of five depth electrodes. A second set of models was also completed that combined data from the UPR-81 SGE survey with the current UPR-86 data.

5.1 INVERSE MODELING RESULTS

This section provides discussions of results of the inverse models. Datasets, both with and without depth electrodes, were modeled for the UPR-86 and extended model area including data collected during previous SGE efforts at the adjacent UPR-81 site.

To create the datasets for inversion, two types of data reduction occurred between the data acquisition and final inversion phases. First, data quality was inspected to eliminate unacceptable data that may have resulted from instrumentation error, electrical interference, or high data misfit with respect to neighboring points. The process of removing spurious data points is referred to as editing and is performed prior to the first inversion run. Secondly, data were filtered after each inverse model was completed to remove data points that contributed to a high model RMS error. This process is referred to as a filter run, and the objective of a filter run was to get the final RMS below 10 percent. At most, one filter run was conducted on the models, with some models requiring no filter runs.

5.1.1 UPR-86 Results

5.1.1.1 Surface to Surface Results. The initial model, Model 001, focused on the 3D data set using only the highest quality measured surface-to-surface (STS) resistivity data, with no depth electrodes. A high quality dataset for inversion was obtained by removing those data with repeat

™ Rock Works is a trademark of Rockware, Inc
® Surfer is a registered trademark of Golden Software, Inc.

errors greater than 2 percent and reciprocal errors greater than 5 percent. After noisy data removal, 73,358 data values remained for inclusion in the model.

A collection of 3D views, rendered from RES3DINV results, are provided in Figure 5-1. These plots show a 3D distribution of resistivity values where the resistivity colors are transparent such that values at multiple resistivity isopleths can be viewed. Specifically, the plots show three resistivity ranges, in log scale, of –0.5 to –0.2 Ohm-meters in red, –0.2 to –0.1 Ohm-meters in yellow, and –0.1 to 0.3 Ohm-meters in green. The plan view Figure 5-1 (A) represents a cumulative spatial distribution of inverted resistivity subsurface conditions, as seen from above. Plot Figure 5-1 (B) shows a view looking east and Figure 5-1 (C) presents an oblique view of the same model.

Figure 5-1. Distribution of Calculated Resistivity for Inverse Model 001.

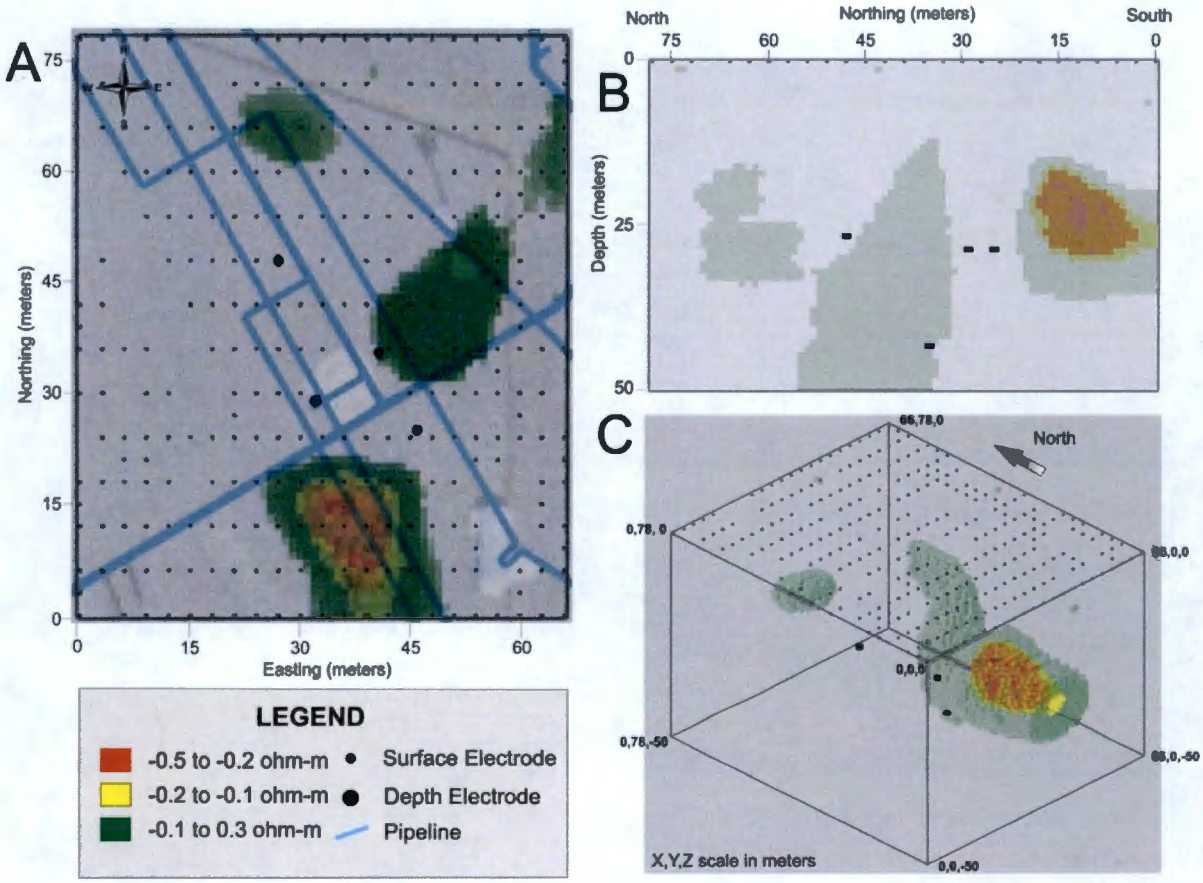

(A) Plan View, (B) Side View, looking East, (C) Oblique View, looking Northeast

In general, the models show a few scattered targets, with the most significant target in the south. The significant target is about 15 meters by 12 meters, and 10 meters in height. The center of the target mass is about 25 meters bgs.

Plan view horizontal depth slices for Model 001, shown in Figure 5-2, present modeling results at increasing depths in meters bgs. The slices are meant to provide more detail regarding the distribution of electrical resistivity in the subsurface.

Figure 5-2. Plan View Depth Slices of Distribution of Calculated Resistivity for Inverse Model 001.

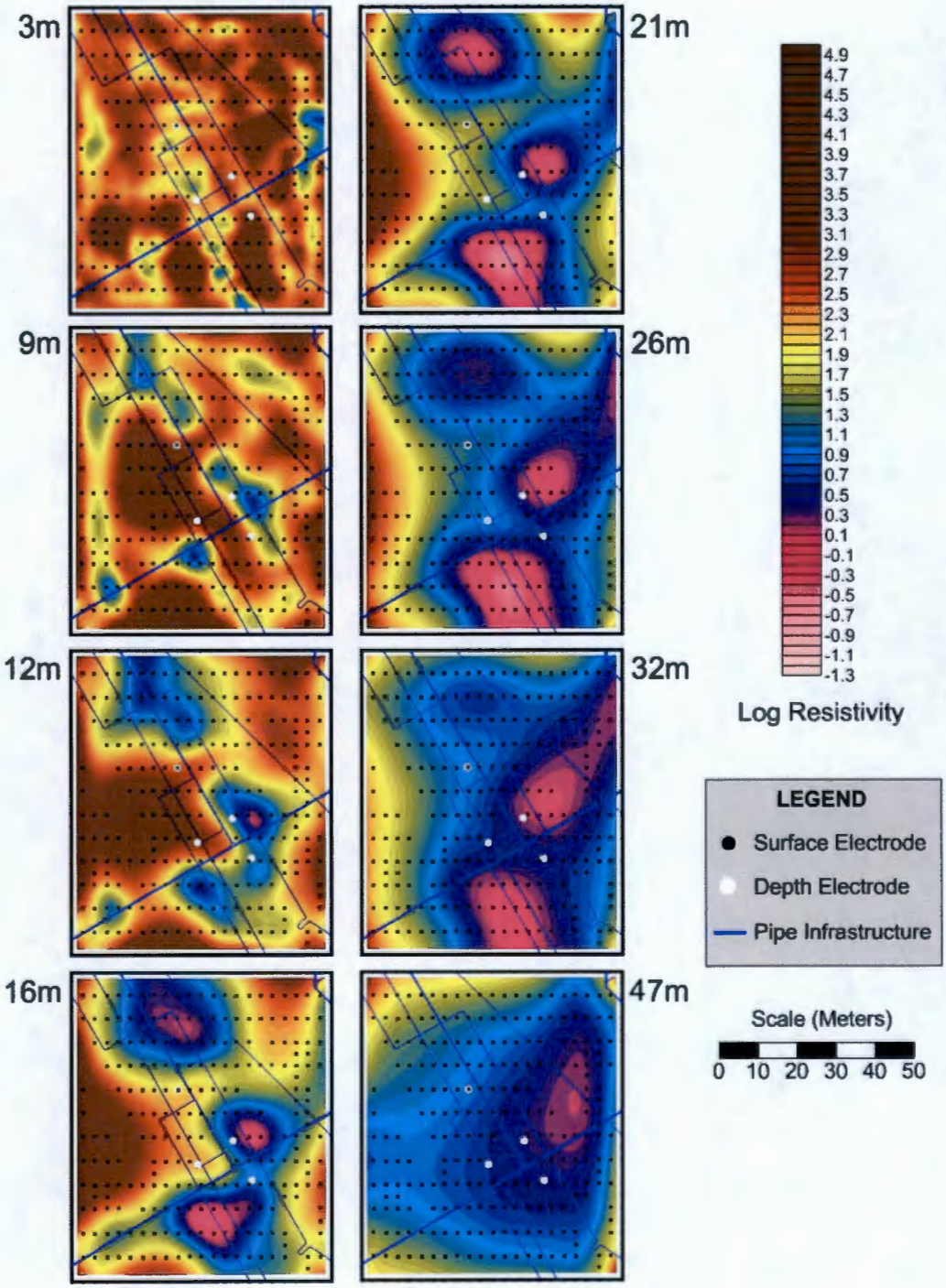

5.1.1.2 Surface-to-Surface with Depth Electrodes. Previous inverse modeling performed at the UPR-81 site showed that those models with depth electrodes had better vertical resolution compared to STS data alone. It was determined that a dramatic improvement could be achieved with even a small quantity of depth electrode data. For the UPR-81 site, only two depth electrodes were used. For the UPR-86 site, there are four available depth electrodes.

Model 019 focused on the 3D data set using both STS and depth electrode resistivity data. This model used the identical STS dataset modeled in Model 001, but also included additional data from the four depth electrodes. After noisy data removal, 75,604 data values remained for inclusion in the model, with 2.6 percent of the data involving depth electrodes either as depth-to-surface or depth-to-depth.

A collection of 3D views, rendered from the RES3DINV results, are provided in Figure 5-3. The plots show three resistivity ranges, in log scale, of –0.5 to –0.2 Ohm-meters in red, –0.2 to –0.1 Ohm-meters in yellow, and –0.1 to 0.3 Ohm-meters in green. The plan view Figure 5-3 (A) represents a cumulative spatial distribution of inverted resistivity subsurface conditions, as seen from above. Plot Figure 5-3 (B) shows a view looking east, and Figure 5-3 (C) presents an oblique view of the same model.

The results of the inversion with depth electrodes show a significantly smaller set of targets compared to the STS data alone. The scattering of the remaining targets, mostly along the perimeter of the model, are reminiscent of noise in the inversion and may not actually represent much in the way of subsurface contamination. The depth electrodes, located deeply beneath the infrastructure, likely provided the additional sensitivity necessary to properly resolve subsurface features.

Further inspection of the raw data show that there are a significant number of STS data values with measured apparent resistivities below the lowest apparent resistivity measured with the depth electrode combinations. The lowest apparent resistivity value for any combination with a depth electrode is 17.36 Ohm-meters. The STS-only dataset has 3,570 values below 17.36 Ohm-meters, with values as low as 11.8 Ohm-meters. The higher values of apparent resistivity from depth electrodes helped increase the overall model resistivity as shown in Figure 5-3. The model results also show that for the STS Model 001, 4.5 percent of the data fall below the 2 Ohm-meters (log value = 0.3 represented by the green isopleths of Figure 5-1), whereas 1 percent fall below 2 Ohm-meters when including the data from depth electrodes.

Figure 5-3. Distribution of Calculated Resistivity for Inverse Model 019.

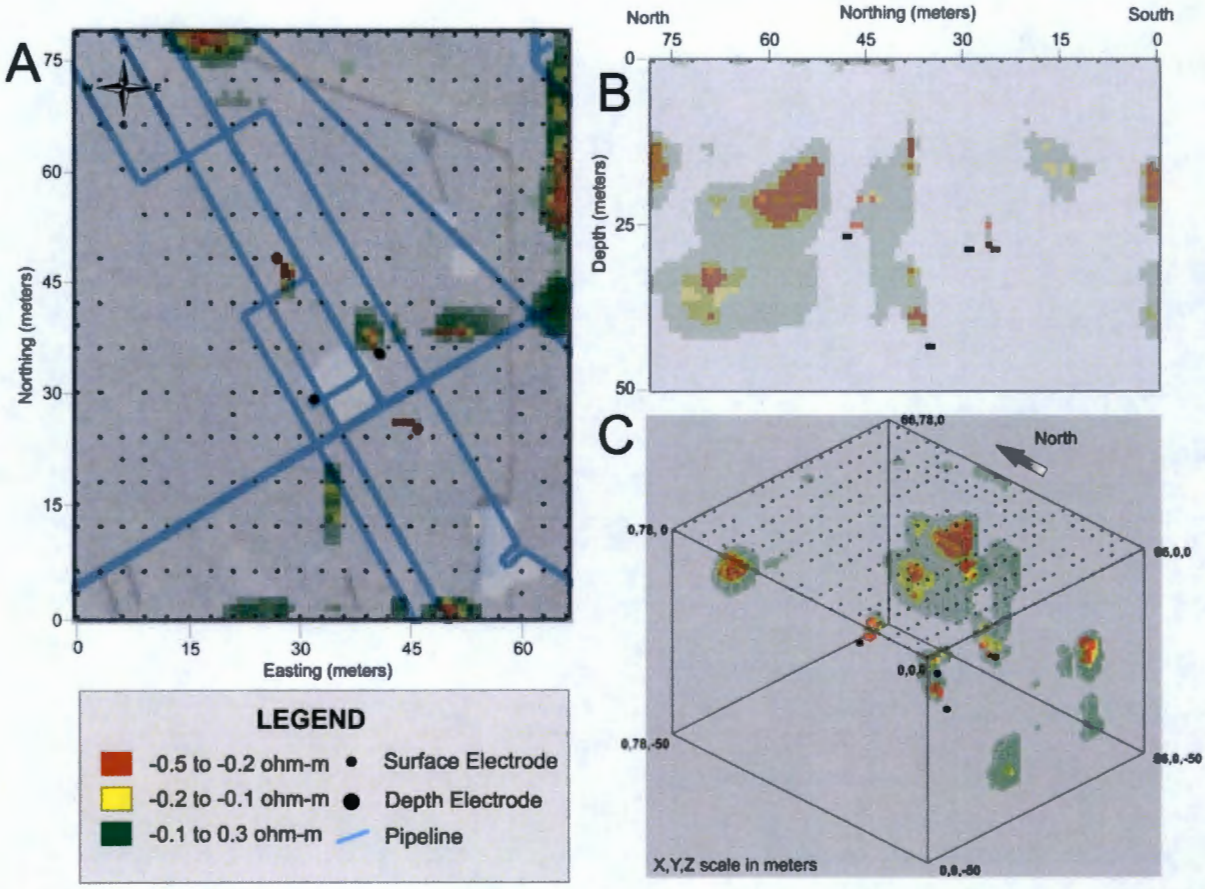

(A) Plan View, (B) Side View, looking East, (C) Oblique View, looking Northeast.

Plan view horizontal depth slices for Model 019, shown in Figure 5-4, presents modeling results at multiple depths in meters bgs.

Figure 5-4. Plan View Depth Slices of Distribution of Calculated Resistivity for Inverse Model 019.

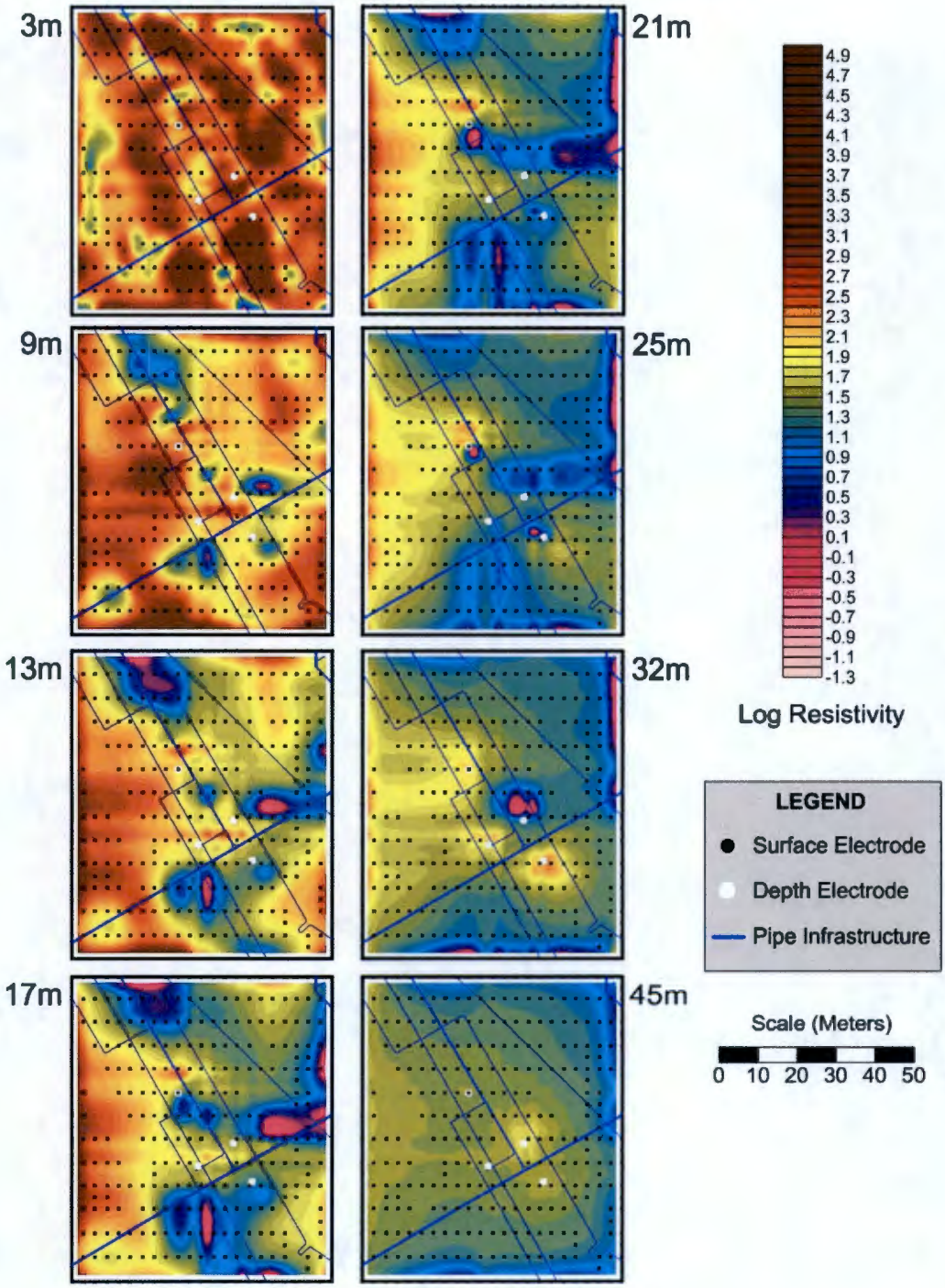

5.1.2 Combined UPR-86 and UPR-81 Data

A set of inverse models were run to evaluate the combined resistivity datasets for UPR-86 and UPR-81. This modeling effort was designed to both explore the results of the current survey more thoroughly, specifically along the eastern edge, and to verify the results based on the degree of continuity of the two models when combined. Figure 5-5 shows the electrode distribution from the UPR-81 and UPR-86 layout, including both surface and depth electrodes in plan view. There were a total 621 surface electrodes and 9 available depth electrodes in the combined projects.

Figure 5-5. Electrode Distribution for the UPR-81 and UPR-86 Resistivity Projects.

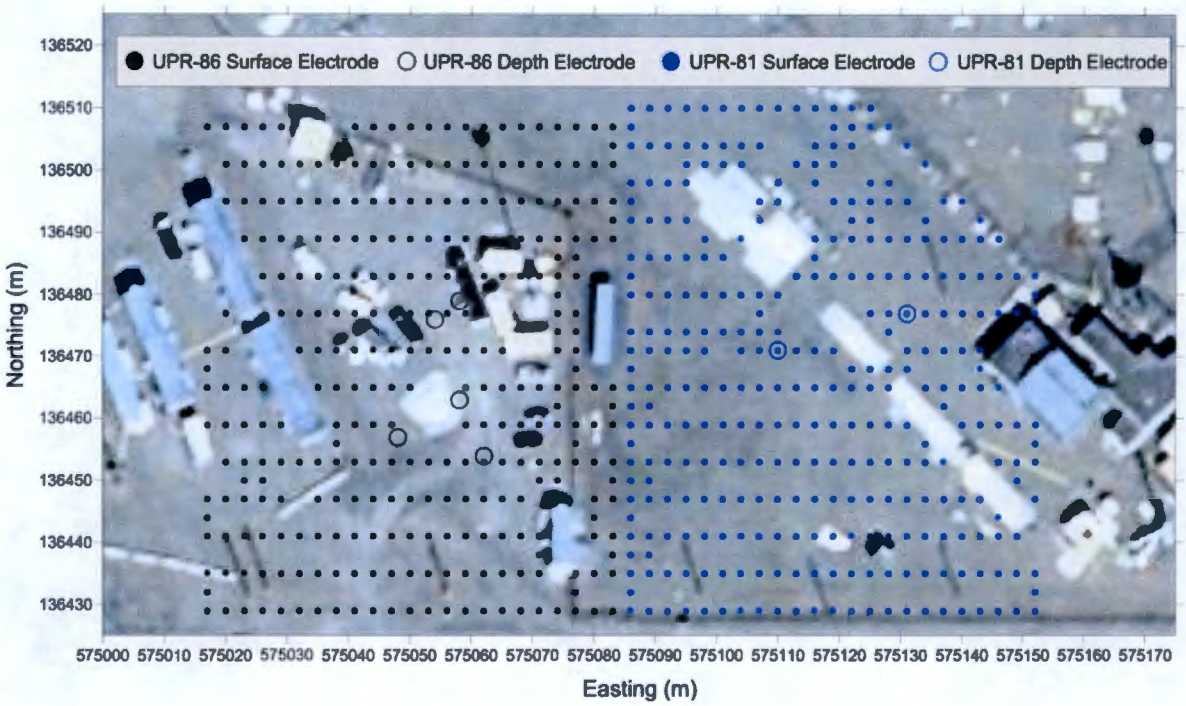

A statistical analysis was performed to compare the two datasets before modeling, and to assess overall data quality. Figure 5-6 displays the results of this analysis as electrical current, repeat error, and transfer resistance (presented as V/I) histograms for STS (column of plots on the left) and depth-to-surface (column of plots on the right). In general, data acquired at UPR-81 displayed an overall lower resistance for both surface and depth electrode data compared to the resistance data at UPR-86. Additionally, the UPR-81 analysis shows that the depth electrode resistance data are lower than the surface data indicating more conductive earth in the deeper subsurface than nearer surface. The UPR-86 resistance data, on the other hand, showed the opposite, that is the depth electrode resistance data were higher than the surface electrode data. Qualitatively, one would expect the inverse model results at the UPR-81site to exhibit lower final resistivity values than the UPR-86 site.

Figure 5-6. Histogram Comparison of the Raw Data for UPR-86 and UPR-81.

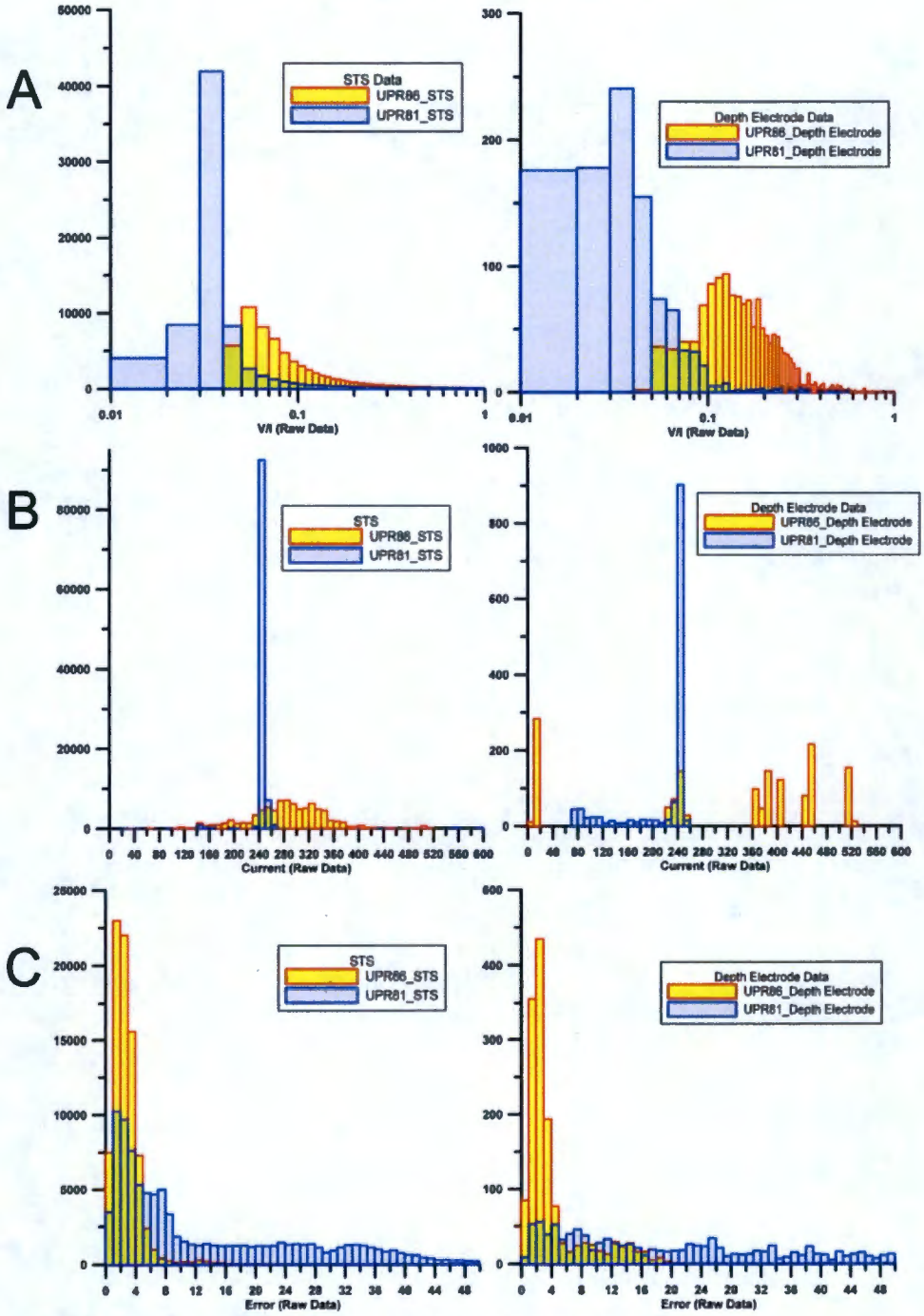

(A) STS (left) and Depth Electrode data (right) V/I (resistance) comparison.

(B) STS (left) and Depth Electrode data (right) Electrical Current comparison.

(C) STS (left) and Depth Electrode data (right) Repeat Error comparison.

STS = surface-to-surface

The electrical current and repeat error data for the UPR-86 project (Figures 5-6 (B) and 5-6 (C)) also appears to be of marginal higher quality than the UPR-81 data set. Higher electrical current output can equate to higher data quality by a reduction in the signal relative to noise. The higher current also indicates a better connectivity to the earth, providing a better suite of voltage measurements. The results of higher current output for UPR-86 is reflected in the repeat error histogram of Figure 5-6(C), where more data tend to be on the lower end of the error scale.

5.1.2.1 Surface to Surface Combined Model Results. Model 024 focused on the combined UPR-86 and UPR-81 3D data set using only the STS resistivity data. Depth electrodes were not included in this model. The input file for Model 024 had a total of 91,833 data values.

A collection of 3D views, rendered from RES3DINV results for Model 024 are provided in Figure 5-7. These plots show a 3D distribution of resistivity values where the resistivity colors are transparent such that values at each resistivity level can be viewed. The plots show three resistivity ranges, in log scale, of –0.5 to –0.2 Ohm-meters in red, –0.2 to –0.1 Ohm-meters in yellow, and –0.1 to 0.3 Ohm-meters in green. The values were kept consistent for direct comparison with Models 001 and 019. The plan view Figure 5-7 (A) represents a cumulative spatial distribution of inverted resistivity subsurface conditions, as seen from above. Plot Figure 5-7 (B) shows a view looking east, and Figure 5-7 (C) presents an oblique view of the same model. The values and viewing angles were kept consistent for direct comparison with Models 001 and 019 in Figures 5-1 and 5-3.

Figure 5-7. Distribution of Calculated Resistivity for Inverse Model 024.

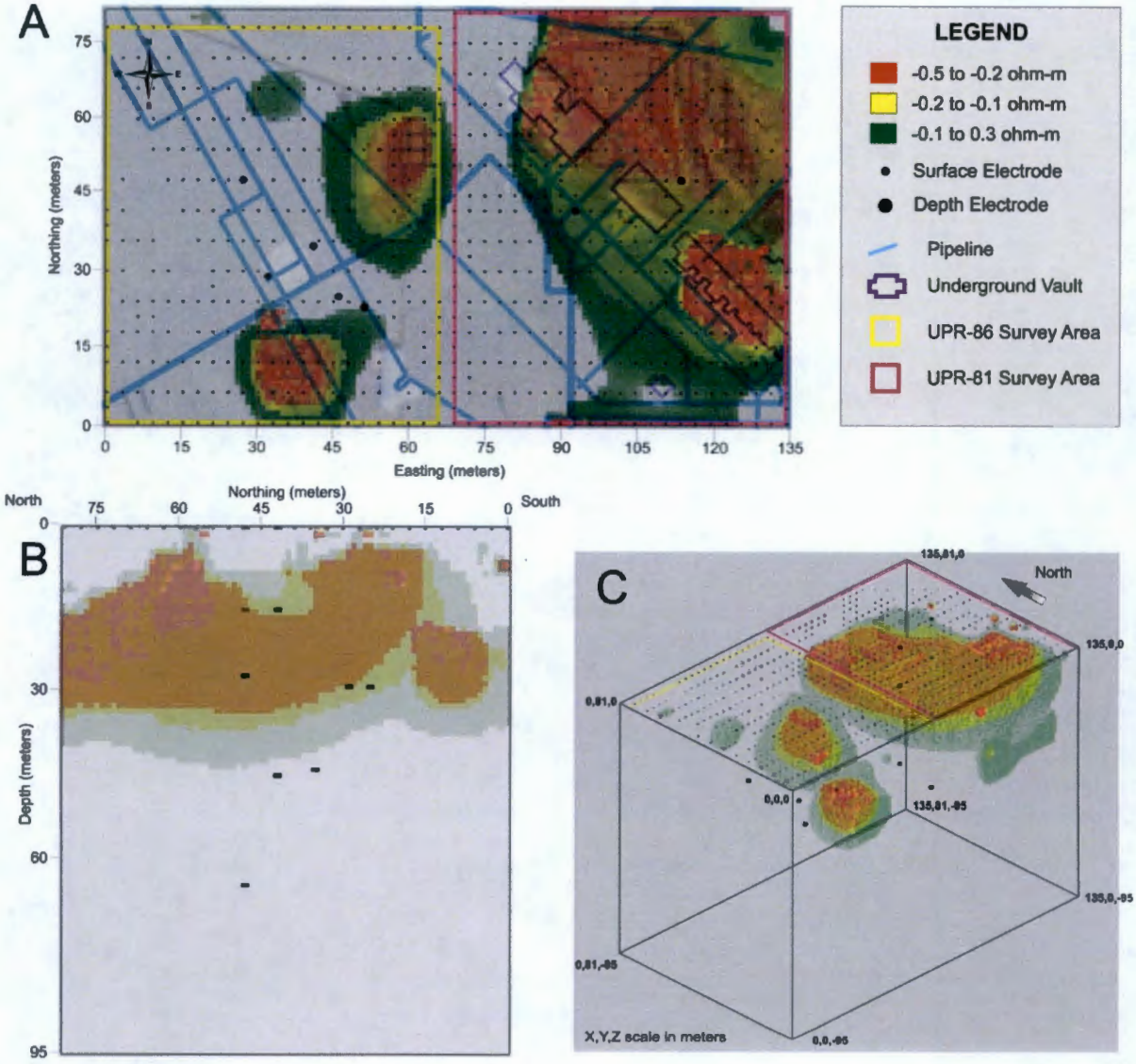

(A) Plan View, (B) Side View, looking East, (C) Oblique View, looking Northeast.

The results show that there are larger targets within the UPR-81domain than in the UPR-86 domain. Given the raw data histograms shown in Figure 5-6, the target distribution was not unexpected. In addition, the targets within UPR-81 are consistent with those presented in the 2009 modeling effort.

Plan view depth slices for Model 024, shown in Figure 5-8, presents modeling results at multiple depths in meters bgs. The center of mass for the low resistivity targets appears to be at a depth of approximately 19 meters.

Figure 5-8. Plan View Depth Slices of Distribution of Calculated Resistivity for Inverse Model 024.

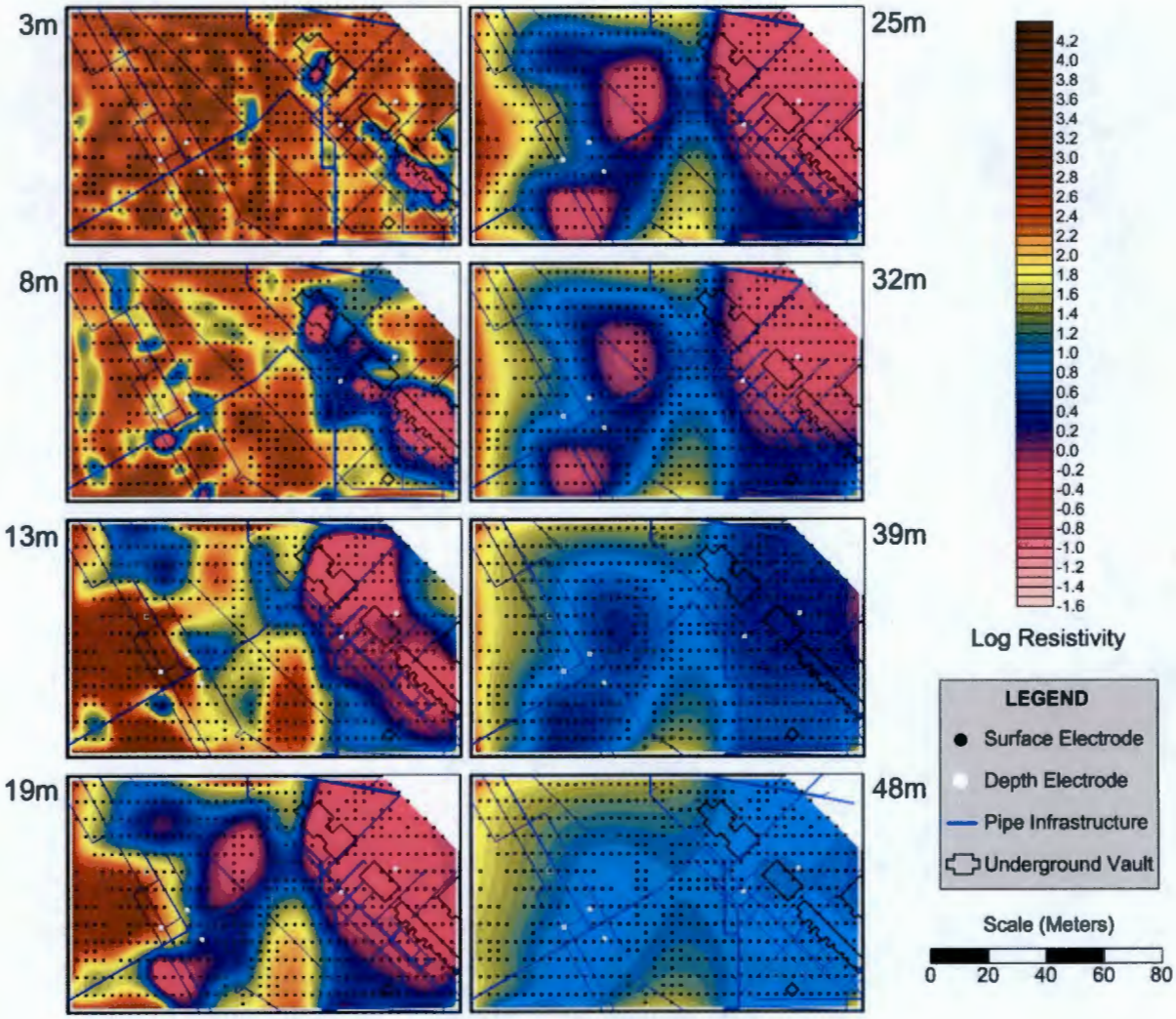

5.1.2.2 Surface to Surface with Depth Electrodes Combined Model Results. Model 025 focused on the combined UPR-86 and UPR-81 3D dataset using both STS and depth electrode resistivity data. Model 025 used the identical STS dataset as Model 024, but also included data from six depth electrodes, four at the UPR-86 site and two at the UPR-81 site. The final data count for Model 025 was 95,252.

A collection of 3D views, rendered from RES3DINV results for Model 024 are provided in Figure 5-9. These plots show a 3D distribution of resistivity values where the resistivity colors are transparent such that values at each resistivity level can be viewed. The plots show three resistivity ranges, in log scale, of –0.5 to –0.2 Ohm-meters in red, –0.2 to –0.1 Ohm-meters in yellow, and –0.1 to 0.3 Ohm-meters in green. The values were kept consistent for direct comparison with Models 001 and 019. The plan view Figure 5-9:

- (A) represents a cumulative spatial distribution of inverted resistivity subsurface conditions, as seen from above.
- (B) shows a view looking east.
- (C) presents an oblique view of the same model.

The values and viewing angles were kept consistent for direct comparison with Models 001 and 019 in Figures 5-1 and 5-3.

Figure 5-9. Distribution of Calculated Resistivity for Inverse Model 025.

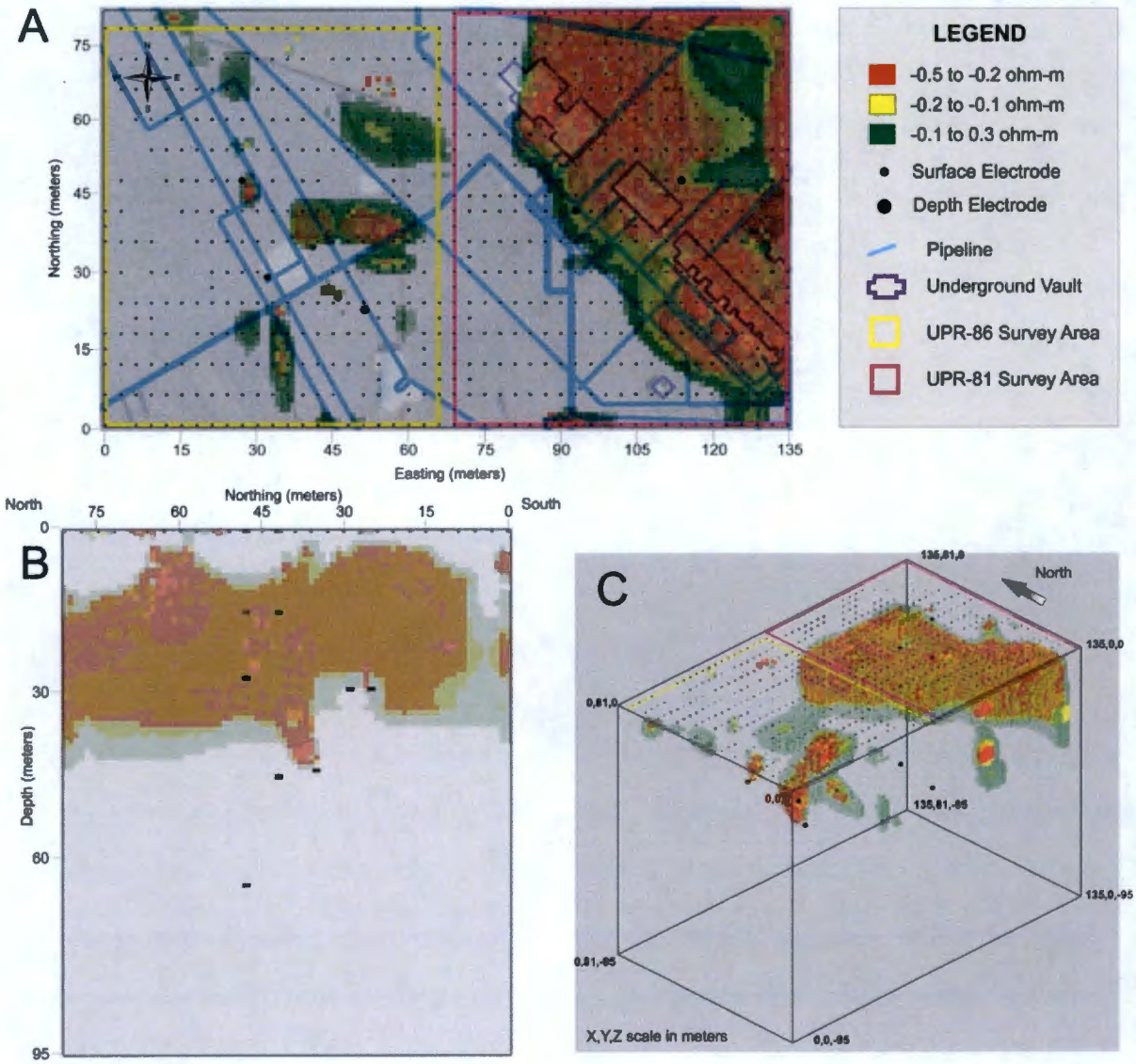

(A) Plan view
(B) Side view, looking east
(C) Oblique view, looking northeast.

Plan view depth slices for Model 025, shown in Figure 5-10, presents modeling results at multiple depths in meters bgs.

Figure 5-10. Plan View Depth Slices of Distribution of Calculated Resistivity for Inverse Model 025.

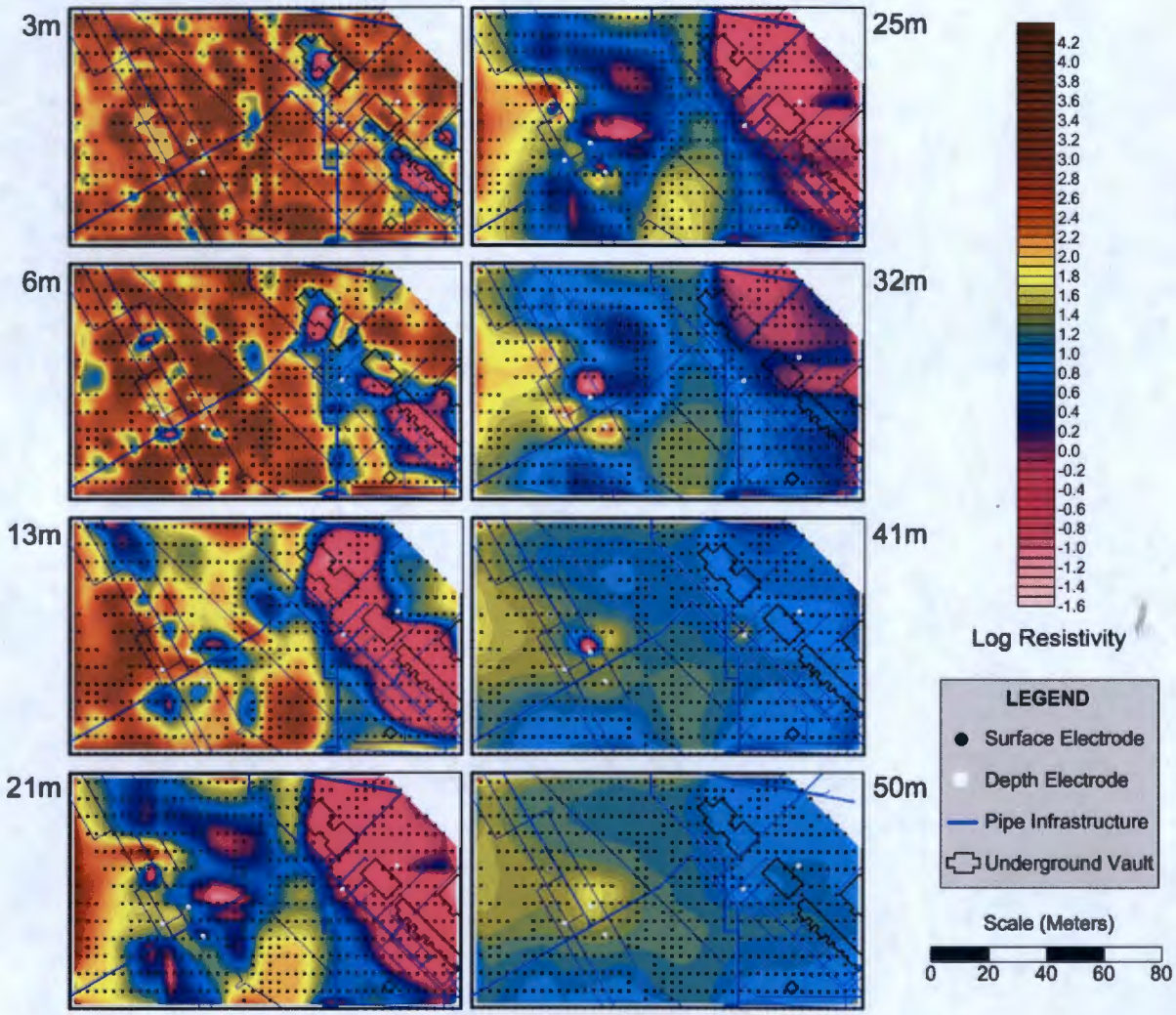

The inversion results for Model 025 shows a large northwesterly oriented, low resistivity target near the underground vaults and minor targets west of the vaults. The depth to the center of mass for the targets around the vault area has decreased from those presented in Model 024, to around 13 meters bgs. The targets within this area are also consistent with those presented in past modeling efforts.

The targets of the UPR-86 area, in the western portion of the site, are much smaller than the UPR-81 area. Given the lower disposal volumes of UPR-86, the targets meet hydrologic expectations.

5.2 MODELING PERFORMANCE

Final models for presentation were chosen based on overall performance and quality of the inversions. A means of assessing the performance of an inversion model was to evaluate the convergence and final model error. Convergence curves present changes in the RMS error versus inversion iteration number. Convergence curves for the final models, Model 001, Model 019, Model 024, and Model 025, are provided in Figures 5-11 through 5-14, respectively.

The RMS error value is an indicator of goodness of fit between the measured data and corresponding calculated values that are provided by RES3DINVx64. It is generally expected that the RMS error should decrease with successive iterations. A deviation from this expected behavior may indicate that the inversion process has become unstable and that isolated high error readings are dominating the model. Additionally, it is normal to see a convergence curve that is not monotonically decreasing for subsequent iterations. Evaluation of the model stability takes the entire trend into consideration.

From a model convergence perspective, all four models were acceptable, but Models 001 and 024 (using only surface electrode data) appear to have produced a more stable solution based on the shape of the resulting convergence curves.

Figure 5-11. Model 001 Convergence Curve.

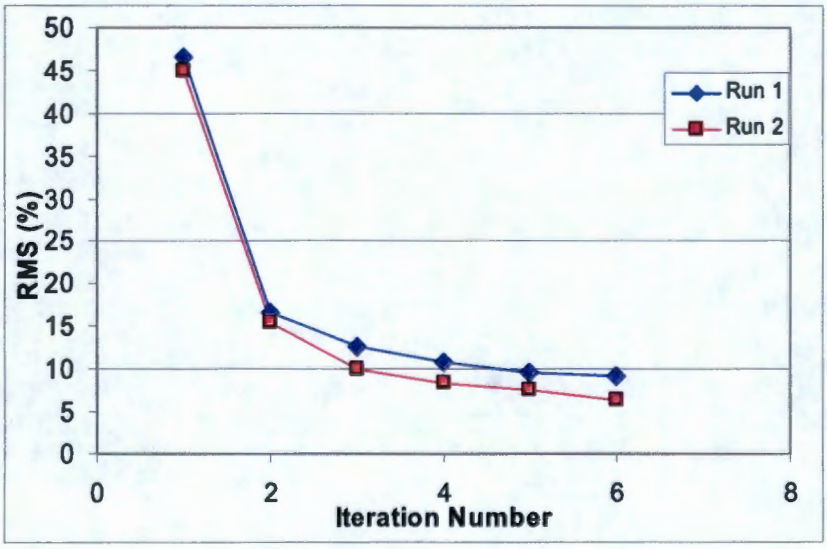

Figure 5-12. Model 019 Convergence Curve.

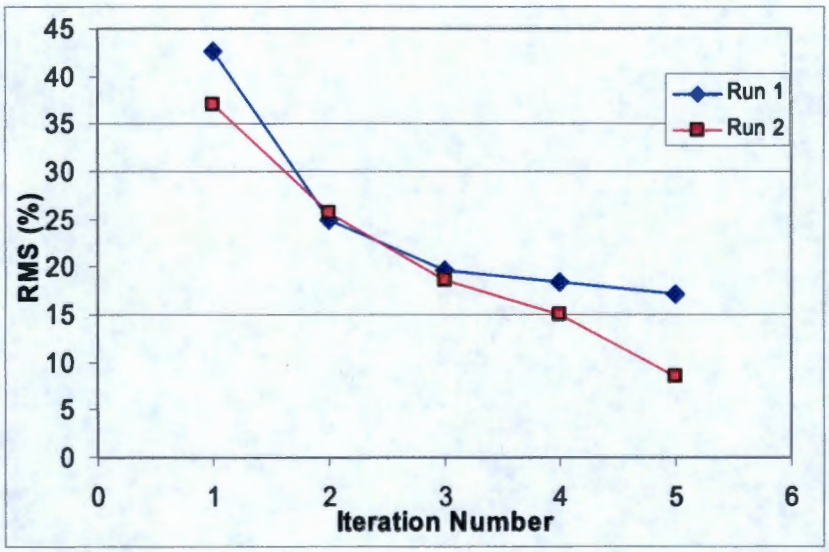

Figure 5-13. Model 024 Convergence Curve.

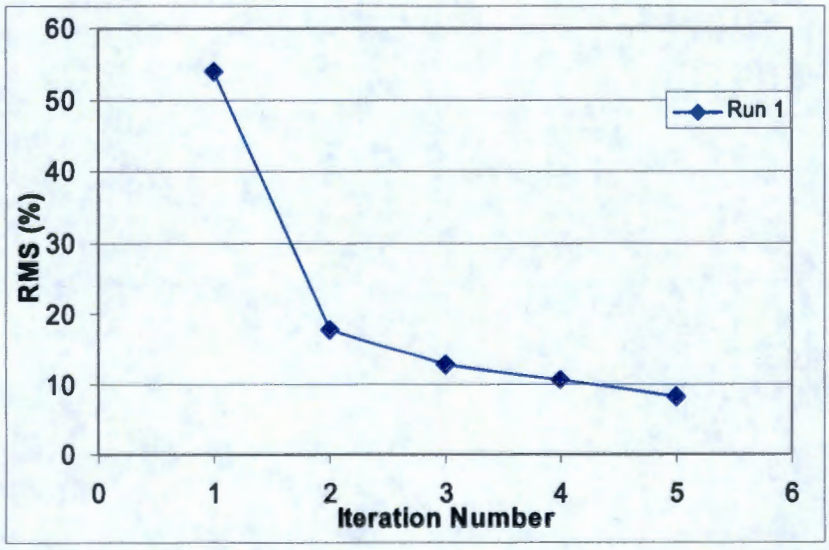

Figure 5-14. Model 025 Convergence Curve.

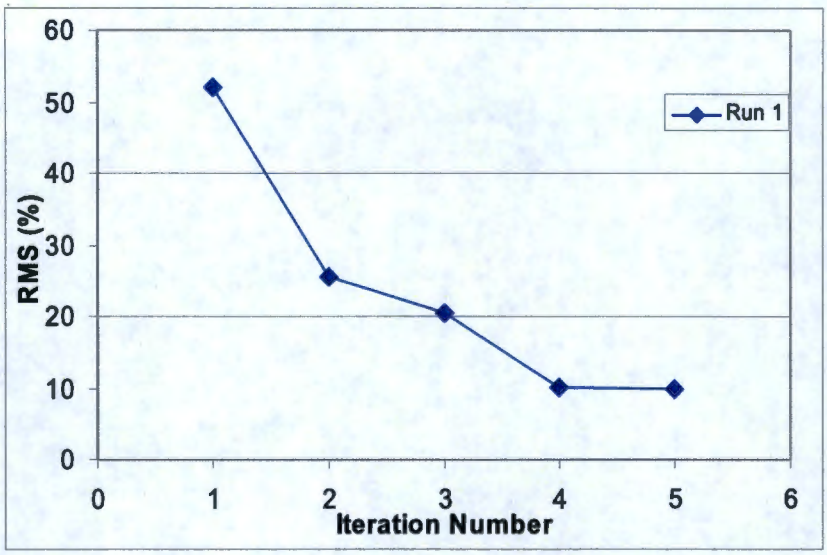

Table 5-1 presents a summary of the data quantity associated with each inversion model and specific electrode set that makes up the dataset.

Table 5-1. Inverse Modeling Convergence and Error Statistics Table.

	Filter Run	Model 001	Model 019	Model 024	Model 025
Number of Data Points	1	73,358	75,604	91,833	95,252
Root-Mean-Square Error (percent)	1	9.2	17.2	8.1	9.8
Number of Data Points	2	69,998	71,872	—	—
Percent Initial Data Remaining	2	95.4	95.1	—	—
Root-Mean-Square Error (percent)	2	6.4	8.5	—	—

6.0 CONCLUSIONS

The primary objective of the C farm UPR-86 survey was to map low-resistivity anomalies that can be evaluated as areas of contamination from past leaks and spills, and potentially guide any direct sampling and analysis activities. In order to meet this objective, electrical resistivity data were acquired with a high-resolution 3D data acquisition method using both surface and depth electrodes. Since it is well known that a substantial amount of metallic infrastructure exists in and around the C tank farm, the survey design for electrode placement incorporated existing engineering drawings to identify preferential locations for the electrodes in areas away from the infrastructure where possible.

Results of the data processing analyses through comparisons of more than thirty separate inverse models identified several key features of the electrical resistivity distribution of the subsurface:

- The depth electrode data proved to be extremely valuable. Their placement below the infrastructure helped increase the level of sensitivity and provided the necessary data to show a relatively resistive subsurface.
- The inverse model using both surface and depth electrode for the UPR-86 site showed only a few scattered low resistivity targets that were reminiscent of noise. These targets tended to be on the periphery of the model domain.
- The more complete inversion that included both UPR-81 and UPR-86 resistivity data showed again that low resistivity targets in the UPR-86 were minimal in comparison to the UPR-81 site.

Based on these findings, the level of release at UPR-86 can be classified as one or more of the following reasons. The list is ordered from most to least probable:

- **The estimated 17,000 gallons released at UPR-86, which is approximately half that of UPR-81, is an overestimate**. It could be that the release volume was actually lower and the 17,000-gallon value was simply an estimate based on a 20-foot by 20-foot by 20-foot block of soil saturated to 30 percent with the spill (8,000 cubic feet times 7.48 gallons per cubic foot times 0.3). If the 17,000-gallon release was a correct estimate, then moisture logs from probeholes close to the spill would likely show some elevated moisture compared to probeholes far from the spill (e.g., C5947 and C5961). However, all moisture logs are fairly uniform showing virtually no signs of the spill.
- **The volume released has been washed through or diluted in the soil by subsequent water addition (natural or anthropogenic).** The dilution hypothesis may have some merit given the nitrate concentrations, as seen in Figure 2-5, are slightly elevated to approximately 15 to 20 ug/g (about 0.5 g/L) at a depth of 25 meters for all of the samples locations. However, assuming a recharge of 0.5 millimeters per year and 30 years since the release, a total length of water added to the soil would be 0.015 meter. If the value of 17,000 gallons for the release is correct, then the length of contaminated water would be approximately 6 meters (20 feet). For one-dimensional plug flow, the dilution factor of 6:0.015 is not sufficient to explain the results from meteoric water alone.

- **The release lacked sufficient ionic strength to provide a suitable target.** Soil samples from around the spill showed low concentrations of sulfate and nitrate compared to other sites around Hanford.
- **The 17,000 gallons was the actual volume released, but occurred over a much broader area such that the resistivity value of the release target blended with the background.** This scenario is unlikely since surface soil contamination would have been found further afield.

The following recommendations are provided to improve future resistivity campaigns in and around the C tank farm:

- Subsurface imaging would likely benefit from additional depth electrodes. The current survey had five depth electrodes available for use, of which four were included into the final modeling. Future surveys using depth electrodes will benefit from the new design that enables the placement of a multiple electrodes installed per drill location.
- With all of the available drilling data (including soil type, ionic constituents, moisture content, porosity), there should be an effort to directly incorporate the information into the inversion model.
- The site could benefit from a much broader coverage of resistivity mapping. It could be the lack of targets for the UPR-86 survey was a result of the entire site acting as a target. The broader resistivity survey could be conducted as a 3D campaign with more and wider spaced electrodes.

7.0 REFERENCES

ASME NQA-1, *Quality Assurance Requirements for Nuclear Facility Applications*, as revised, American Society of Mechanical Engineers, New York, New York.

ASME NQA-1, Subpart 2.7, "Quality Assurance Requirements for Computer Software for Nuclear Facility Applications," as revised, American Society of Mechanical Engineers, New York, New York.

CE-ES-3.5, *Software Engineering*, as revised, Columbia Energy and Environmental Services, Inc., Richland, Washington.

CEES-0333, 2006, *Quality Assurance Plan for Surface Geophysical Exploration Projects*, as revised, Columbia Energy and Environmental Services Inc., Richland, Washington.

CEES-0338, 2006, *Software Management Plan for Surface Geophysical Exploration Projects*, Columbia Energy and Environmental Services Inc., Richland, Washington.

CEES-0360, 2007, *Surface Geophysical Exploration System Design Description*, Revision 0, Columbia Energy and Environmental Services Inc., Richland, Washington.

Contract 28090, Requisition 123974, *High Resolution Resistivity Characterization of Single Shell Tank Farm Waste Management Areas* Revision 3, CH2M HILL Hanford Group, Inc., Richland, Washington.

DOE O 414.1C, *Quality Assurance*, U.S. Department of Energy, Washington, D.C. Available at: http://www.directives.doe.gov/pdfs/doe/doetext/neword/414/o4141c.pdf.

DOE/ORP-2003-11, 2003, *Preliminary Performance Assessment for Waste Management Area C at the Hanford Site, Washington*, Revision 0, CH2M HILL Hanford Group, Inc., Richland, Washington.

DOE/RL-92-04, 1993, *PUREX Aggregate Area Management Study Report [AAMSR]*), Revision 0, U.S. Department of Energy, Richland Operations Office, Richland, Washington.

DOE/RL-92-24, 1995, *Hanford Site Background: Part 1, Soil Background for Nonradioactive Analytes*, Revision 4, U.S. Department of Energy, Richland Operations Office, Richland, Washington.

Gharibi, M., and L.R. Bentley, 2005, "Resolution of 3-D Electrical Resistivity Images from Inversions of 2-D Orthogonal Lines," *Journal of Environmental and Engineering Geophysics*, Volume 10(4):339-349.

PNNL-SA-60937, 2008, *Geochemical Characterization of Sediments from UPR 200-E-86*. Pacific Northwest National Laboratory, Richland, Washington

PNNL-SA-61511, 2008, *Geochemical Characterization of Sediments from UPR 200-E-81*. Pacific Northwest National Laboratory, Richland, Washington

RPP-14430, 2003, *Subsurface Conditions Description of the C and A-AX Waste Management Areas*, Revision 0, CH2M HILL Hanford Group, Inc., Richland, Washington.

RPP-34690, 2007, *Surface Geophysical Exploration of the B, BX, and BY Tank Farms at the Hanford Site*, Revision 0, CH2M HILL Hanford Group, Inc., Richland, Washington.

RPP-RPT-35104, 2007, *Verification and Testing of the EarthImager Series of Electrical Resistivity Inversion Codes – A Benchmark Comparison*, Revision 0,CH2M HILL Hanford Group, Inc., Richland, Washington.

RPP-35484, 2007, *Field Investigation Report for Waste Management Areas C and A-AX*, Revision 1, CH2M HILL Hanford Group, Inc., Richland, Washington.

RPP-PLAN-39114, 2010, *Phase 2 RCRA Facility Investigation/Corrective Measures Study Work Plan for Waste Management Area C*, Revision 1, Washington River Protection Solutions, LLC, Richland, Washington.

RPP-PLAN-39364, 2010, *Work Plan for Surface Geophysical Exploration of UPRs near the C-Tank Farm*, Revision 2, Washington River Protection Solutions, LLC, Richland, Washington, Richland, Washington.

RPP-RPT-41236, 2009, *Surface Geophysical Exploration of UPR 200-E-81 Near the C Tank Farm*, Revision 0, Washington River Protection Solutions, LLC, Richland, Washington.

RPP-RPT-42294, 2010, *Hanford Waste Management Area C Soil Contamination Inventory Estimates*, Revision 1, Washington River Protection Solutions, LLC, Richland, Washington.

RPP-RPT-42844, 2009, *Reanalysis of Surface Geophysical Exploration Resistivity Data for the 241 T Tank Farm*, Revision 0, Washington River Protection Solutions, LLC, Richland, Washington.

Rucker, D.F., M.T. Levitt, and W.J. Greenwood, 2009. "Three-dimensional Electrical Resistivity Model of a Nuclear Waste Disposal Site." *Journal of Applied Geophysics* 69:150-164.

Yang, X., and Lagmanson, M., 2006, *Comparison of 2D and 3D Electrical Resistivity Imaging Methods, Symposium on the Application of Geophysics to Engineering and Environmental Problems*, Environmental and Engineering Geophysical Society (EEGS), Seattle, Washington.